Infection and Inflammation of the Musculoskeletal System

31

Hee Kyung Kim

Contents

H.K. Kim, M.D.
Department of Radiology, Cincinnati Children's Hospital
Medical Center, 3333 Burnet Avenue, Cincinnati, OH 45229, USA
e-mail: hee.kim@cchmc.org

I.-O. Kim (ed.), *Radiology Illustrated: Pediatric Radiology*, Radiology Illustrated,
DOI 10.1007/978-3-642-35573-8_31,

31.1 Introduction

This chapter will describe various infectious and inflammatory disorders of the musculoskeletal system in children. Familiarity with characteristic imaging findings of infectious and inflammatory disorders will enable a more confident and accurate differential diagnosis. Some infectious musculoskeletal disorders, including pyogenic osteomyelitis and septic arthritis, are acute processes for which early diagnosis and prompt treatment are critical, while others, such as tuberculous arthritis, are more insidious. Inflammatory arthritis and chronic recurrent multifocal osteomyelitis are sterile inflammatory disorders with multiple joint and bone involvement. Other types of inflammatory arthritis may be associated with underlying disease, such as hemophilic arthropathy and neuropathic arthritis. Miscellaneous joint disorders, including pigmented villonodular synovitis, synovial osteochondromatosis, lipoma arborescens, leukemic arthritis, and synovial vascular malformation, are rare in children but can present with joint pain mimicking inflammatory arthritis. Imaging plays an important role in evaluation of all of these disorders. Plain radiographs are the first step in initial evaluation. Ultrasound exam is useful for evaluation of joint effusion and soft tissue abnormalities. MR imaging offers superior tissue contrast and often requires sedation.

31.2 Infectious Disorder of the Bone and Joint

31.2.1 Pyogenic Osteomyelitis

31.2.1.1 Acute Osteomyelitis

Osteomyelitis is an infection of the bone and bone marrow. There are three routes of spread of infection: hematogenous, direct implantation, and contiguity. In hematogenous spread of infection, the metaphysis of the long bones are primarily affected.

Imaging evaluation can be performed with plain radiographs as first step. In early osteomyelitis, soft tissue swelling may be seen, but periosteal reaction and bone destruction are usually not appreciated until at least 7–10 days after disease onset (Fig. 31.1). Bone scintigraphy (bone scan) is useful in initial assessment and localization of the infectious/inflammatory process in osteomyelitis because it has high sensitivity (82 %). Increased uptake within the involved bone at all three phases (angiographic, blood pool, and 2 h delayed bone phases) is suggestive of osteomyelitis (Fig. 31.1). In acute osteomyelitis, MR imaging demonstrates an ill-defined area of low T1 and high T2 bone marrow signal reflecting edema. Intramedullary exudates and a poorly demarcated area of soft tissue swelling are also observed (Fig. 31.1). Post-contrast T1-weighted imaging (WI) is the best sequence on which to detect an abscess, which is demonstrated by localized fluid signal with rim enhancement (Fig. 31.1). A poor demarcation between abnormal and normal bone marrow is an excellent predictor of acute osteomyelitis and can differentiate it from chronic osteomyelitis or neoplasm of the bone. Ultrasound is adequate to evaluate periosteal fluid collection or abscess; periosteal elevation by an anechoic zone of more than 2 mm is a characteristic sign of subperiosteal abscess (Fig. 31.2) and requires prompt surgical drainage (Howard et al. 1993).

31.2.1.2 Brodie's Abscess

Brodie's abscess is seen in subacute osteomyelitis as a radiolucent area with well-circumscribed sclerosis (Fig. 31.3).

31.2.1.3 Sclerosing Osteomyelitis and Sequestration

Dense cortical thickening is a finding of chronic osteomyelitis that may be seen months or years after infection and is known as Garré sclerosing osteomyelitis (Fig. 31.4). Cortical extension of infection results in an area of sequestration of a vascular bone surrounded by pus and thickened bone, called a sequestrum (Fig. 31.5).

31.2.2 Septic Arthritis

Septic arthritis is one of the disease entities that require urgent surgical intervention to avoid devastating destructive joint changes. In infants and children less than 18 months of age, the metaphyses and epiphyses of the long bones are cosupplied by a transphyseal vessel. The transphyseal vessels allow the spread of infection into the epiphysis and joints in these young children.

When there is clinical suspicion of septic arthritis, initial imaging evaluation is focused on the presence of joint effusion, not definitive diagnosis of septic arthritis. The absence of joint effusion is an important finding that can exclude septic arthritis with high accuracy (100 % negative predictive value) (Hopkins et al. 1995). Presence of a significant joint effusion with synovial thickening is a sign of underlying inflammation, which can be seen in noninfectious (sterile) inflammatory synovial disease as well as septic arthritis (Fig. 31.6) (Hopkins et al. 1995).

On plain radiographs, joint effusions of the knee, ankle, and elbow (Fig. 31.6) can be detected. However, plain radiographs are limited in the evaluation of joint effusions of the hip, shoulder, and sacroiliac joints, which are better evaluated with ultrasound, CT, or MR imaging. Differentiation of septic arthritis from noninfectious inflammatory arthritis is difficult on any imaging modality. On ultrasound exam, neither the size nor echogenicity of joint effusion enables correlation with sterility of joint effusion (Jaramillo et al. 1995). On MR exam, the presence of bone marrow edema in septic arthritis of the hip was shown to be useful in the differentiation of transient synovitis in one study (Lee et al.

1999). However, bone marrow edema is seen in osteomyelitis as well as in reactive changes in noninfectious conditions, and therefore differentiation of those entities is difficult.

Soft tissue or intraosseous abscess formation, cartilage and bone erosion, and destructive changes (Fig. 31.7) are seen as secondary changes related to septic arthritis.

If joint effusion is detected in a patient with clinical suspicion of septic arthritis, prompt diagnostic aspiration of the effusion should be performed to exclude septic arthritis (Kan et al. 2010).

31.2.3 Tuberculous Arthritis

Tuberculous (TB) arthritis usually results from hematogenous spread of *Mycobacterium tuberculosis*; musculoskeletal involvement is found in approximately 1–3 % of all TB infections and is more common in children. Diagnosis of TB arthritis can be delayed due to its insidious onset and indolent disease course. Plain radiographs demonstrate joint effusion in 3–4 weeks after disease onset. Later manifestations include joint space narrowing, erosion, and destruction. Phemister's triad of periarticular osteoporosis, gradual joint space narrowing, and osseous erosion is the classic finding of TB arthritis. Unlike pyogenic arthritis, which has rapid joint space destruction, joint space is relatively preserved in many patients with TB arthritis. Bone erosion resulting from the proliferation of granulation tissue occurs over a longer time course (Fig. 31.8). MR imaging demonstrates joint effusion with occasional rice bodies, synovitis, tenosynovitis, and cortical erosions. However, these findings are not specific for TB arthritis. Based on imaging alone, differentiation TB arthritis from inflammatory or pyogenic arthritis is still difficult. In TB arthritis, extra-articular abscess formation and bone erosions with rim enhancement are more common than noninfectious inflammatory arthritis (Choi et al. 2009). Lack of bone marrow edema and an abscess with thin, smooth margins may be useful to differentiate TB arthritis from pyogenic arthritis. In pyogenic arthritis, bone marrow edema is more commonly seen, and an abscess has more irregular and relatively thick walls (Burk et al. 1988). Another sign that is more suggestive of TB arthritis is a tram track appearance resulting from a linear fluid signal from the joint space with rim enhancement (Fig. 31.9) (Parmar et al. 2004). However, due to overlap between imaging findings of TB arthritis, noninfectious inflammatory arthritis, and pyogenic arthritis, it is important to pursue cultures of synovial fluid and synovium (Erdem et al. 2005).

31.2.4 Congenital Syphilis

Congenital syphilis is a transplacental infection due to *Treponema pallidum* that occurs during the second to third trimesters of gestation. Plain radiographs in infants with congenital syphilis demonstrate multiple bone involvement with metaphyseal lucent bands and periosteal new formation of the diaphysis (Fig. 31.10). These findings reflect stress responses and can be seen in other disseminated infections. A focal area of destructive changes in the medial aspect of the proximal tibial metaphysis with preservation of a few millimeters of recently formed metaphysis (Laval-Jeantet collar) is called "Wimberger's sign" (Fig. 31.10). Wimberger's sign is strongly suggestive of congenital syphilis, and diagnosis is made in conjunction with serologic testing.

31.3 Infectious Disorders of the Soft Tissue

31.3.1 Pyomyositis

Pyomyositis is a bacterial infection of the skeletal muscle that mainly affects children between 2 and 5 years. It is more common in tropical areas; however, the incidence is increasing in temperate areas. Pyomyositis is characterized by abscess within the muscles, often following minor trauma. MR imaging shows localized fluid signal with peripheral rim enhancement within the muscle suggesting abscess and can be associated with cellulitis, myositis, and fasciitis (Fig. 31.11) (Gordon et al. 1995).

31.4 Noninfectious Inflammatory Diseases of the Bones and Joints

31.4.1 Inflammatory Arthritis

31.4.1.1 Juvenile Idiopathic Arthritis

Juvenile idiopathic arthritis (JIA) is the most common inflammatory arthritis. It is diagnosed in children under age 16 years who have more than 6 weeks of symptom duration. JIA is classified into seven categories based on the number and types of the involved joints and combined symptoms (Petty et al. 2004). Oligo- or pauci-articular arthritis, with less than five joints involved, is the most common type and accounts for 50–60 % of JIA. It is subclassified based on duration and extension of disease: persistent type (<6 months of duration) versus extended type (>6 months of duration) (Weiss and Ilowite 2007). Systemic and polyarticular arthritis types have more than five joints involved. The systemic type accounts for 10–20 % of JIA and is typically seen in children younger than 5 years. Systemic arthritis is associated with systemic symptoms including spiking fevers, lymphadenopathy, rash, hepatosplenomegaly, and serositis (Weiss and Ilowite 2007). Polyarticular arthritis is subclassified by the presence of rheumatoid factor (RF) into RF positive type, which is less common and similar to adult onset rheumatoid arthritis, and RF negative type, which is

more common. The remaining types of JIA include psoriatic arthritis (2–15 %), enthesitis-related arthritis (1–7 %), and undifferentiated arthritis. Juvenile ankylosing spondylitis and inflammatory bowel disease-related arthropathy are subtypes of enthesitis-related arthritis (Weiss and Ilowite 2007).

The etiology of JIA is an immune response cascade initiated by infection in an immunologically susceptible individual. The primary pathology is synovial inflammation and hypertrophy resulting from cross-reaction of the antigen–antibody to the synovial membrane. The disease is progressive and results in cartilage or bone erosion with eventual joint deformities observed in approximately one-third of affected patients.

Imaging findings on plain radiographs depend on disease stage. In early stages, soft tissue swelling, periarticular osteopenia, joint effusion, and periosteal reaction are seen. Persistent hyperemia results in accelerated skeletal maturation and squaring of the carpal bones. In more advanced stages, joint space narrowing, erosions, and ultimately ankylosis are observed (Fig. 31.12). The knee joint (Fig. 31.13) is most commonly involved, followed by ankle, wrist, hand, shoulder, cervical spine (Fig. 31.14), temporomandibular joint (Fig. 31.15), and sacroiliac joint.

MR imaging with intravenous gadolinium injection is better than plain MR imaging in the evaluation of cartilage erosion and synovial hypertrophy and can demonstrate the most characteristic findings of JIA, which are synovial hypertrophy and joint effusion. In the knee joint, synovial thickening more than 3 mm is considered abnormal. The thickened synovium has variable signal intensities on T1- and T2-WI (Gylys-Morin et al. 2001).Chronic inflammation and fragmentation of synovium results in rice bodies in the joint spaces (Fig. 31.13). Hypoplastic menisci from mass effect of the adjacent thickened synovium, popliteal cysts, lymphadenopathy, and tenosynovitis can also be seen in JIA.

31.4.1.2 Juvenile Spondyloarthropathies

Juvenile spondyloarthropathies is a group of disorders that includes juvenile ankylosing spondylitis, reactive arthritis (Reiter's syndrome), juvenile psoriatic arthritis, and arthritis associated with inflammatory bowel disease. These diseases occur under the age of 16 years and have the common imaging findings of sacroiliitis and enthesitis. The other joint involvement and findings are similar to JIA. Bilateral and asymmetric sacroiliitis with erosions, reactive sclerosis (particularly on the iliac side), pseudo-widening, and indistinct margin are best evaluated on MR imaging with intravenous contrast (Fig. 31.16).

31.4.1.3 Chronic Recurrent Multifocal Osteomyelitis

Chronic recurrent multifocal osteomyelitis (CRMO) is a sterile inflammatory bone disorder. It has recently been considered a hereditary disorder or another manifestation of an associated autoimmune disorder. CRMO primarily affects children from 4 to 14 years with female predominance. The clinical presentation of CRMO is prolonged (over several years), with recurrent and multifocal pain, swelling, and occasional fever. It is often misdiagnosed or simply treated with anti-inflammatory medicines. The metaphyses of the long bones are most commonly involved, followed by the clavicles and spine, and bilateral involvement is common (Fig. 31.17). Bone scan can be used as an initial exam to detect multifocal bone involvement (Fig. 31.18). Plain radiographs demonstrate mixed sclerotic and lytic lesions within the metaphyses of the long bones (Fig. 31.17). On MR images, bone marrow edema is visualized in the active disease state, but in contrast to subacute or chronic osteomyelitis, abscess formation is not observed (Fig. 31.18). In the reparative state, destructed bones demonstrate healing with sclerosis, remodeling, and normalization, which occur within 2 years after disease onset. Subsequent exacerbations with a repetitive cycle of active and reparative states result in progressive hyperostosis and sclerosis of the metaphysis (Fig. 31.18). Diagnosis of CRMO is primarily made by exclusion of other infectious, inflammatory etiologies or neoplasms, and biopsy with histological confirmation is often required (Iyer et al. 2011). SAPHO (*s*ynovitis, *a*cne, *p*ustulosis, *h*yperostosis, and *o*steitis) is a term used to unify idiopathic inflammatory and infectious disorders of bone and skin.

31.4.2 Other Noninfectious Inflammatory Joint Diseases

31.4.2.1 Transient Synovitis

Transient synovitis is an inflammatory synovitis affecting the hip joint that is self-limited in nature. This entity is described in the chapter on hip joint disorders.

31.4.2.2 Hemophilic Arthropathy

Hemophilia is an X-linked autosomal recessive blood coagulation disorder resulting from a lack of coagulation factor VIII or IX. Hemophilic arthropathy is related to repeated intra-articular hemorrhage (hemarthrosis) occurring spontaneously or due to minor trauma. Hemarthrosis accounts for most bleeding events (85 %) in hemophilia and begins in the first and second decades of life. The knee, elbow, ankle, hip, and shoulder joints are most commonly involved. Recurrent

hemarthrosis and hyperemia lead to synovitis, overgrowth of the epiphysis, and eventual degeneration of the joints. Imaging findings are dependent on the disease state and can be graded using the Arnold-Hilgartner staging on plain radiograph: Stage 0, normal; 1, joint effusion and soft tissue swelling; 2, periarticular osteopenia and overgrowth of the epiphysis; 3, bone erosion and widening of the notch of the distal humerus and femur; 4, joint space narrowing (Fig. 31.19); and 5, joint contracture and deformity (Arnold and Hilgartner 1977; Luck et al. 2004).

MR imaging is very useful to detect early changes such as hemarthrosis (blood clot in the joint, fluid–fluid level) and cartilage erosion. Hemosiderin deposition results in characteristic low T1 and low T2 signal within the thickened synovium, which can be best seen on gradient echo sequences (Fig. 31.19) (Kerr 2003; Doria 2010). In advanced stages, degenerative changes including subchondral cysts, cartilage thinning, or erosions can be seen (Fig. 31.19).

31.4.2.3 Neuropathic Arthritis

Neuropathic arthritis is a joint destructive disorder secondary to repetitive trauma over long time period. This is frequently seen in patients with neurosensory loss such as with myelomeningocele or syringomyelia. Plain radiographs demonstrate progressive fracture and dislocation of the joint (Fig. 31.20). MR findings of neuropathic joint include fragmentation of the cartilage and bones, synovial thickening, effusion, and ligament and menisci injuries. Lack of inflammation in the periarticular space in the neuropathic joint and an underlying history of neuropathy can be helpful to differentiate it from pyogenic arthritis.

31.4.3 Miscellaneous Disorder of the Joint

31.4.3.1 Pigmented Villonodular Synovitis

Pigmented villonodular synovitis (PVNS) is an idiopathic proliferative disorder of the synovium. It is relatively rare in children and has a benign course in most cases. The knee is most frequently involved (80 %) followed by the hip, ankle, shoulder, and elbow joints. PVNS has two types: diffuse PVNS is more common and involves the entire synovium of the affected joint, and localized PVNS is less common and can mimic a fibrous neoplasm. Giant cell tumor and benign giant cell synovioma are other names for localized PVNS. Microscopically, the affected synovium has villonodular proliferation with hemosiderin deposition. Plain radiographs show soft tissue swelling with or without degenerative arthritis (Fig. 31.21). The larger joints (knees and shoulders) are preserved from degenerative changes, but tight joints such as the hip can have degenerative changes with joint space narrowing later (Dorwart et al. 1984; Goldman and DiCarlo 1988). MR imaging has a characteristic appearance with low T1 and low T2 signal lesions; diffuse PVNS has diffuse linear or frond-like proliferation of the synovium (Fig. 31.21), and localized PVNS has a localized mass (Fig. 31.22). Gradient echo sequences are useful to differentiate PVNS from other fibrous lesions (synovial hypertrophy with fibrosis in JIA or fibrous tumor). On gradient echo sequences, hemosiderin deposition causes blooming from susceptible artifact (Llauger et al. 1999). PVNS is treated by surgical resection, but the local recurrence rate is relatively high at up to 50 %.

31.4.3.2 Synovial Osteochondromatosis

Synovial osteochondromatosis is an idiopathic synovial proliferative disease with the formation of intrasynovial chondro-osseous bodies. It is relatively rare in children and has a benign nature with single-joint involvement. Three phases of the disease process have been described: *active phase* with chondral proliferation in the synovium without intra-articular loose bodies, *transitional phase* with both intrasynovial chondral proliferation and formation of intra-articular loose bodies, and *quiescent phase* with ceasing of chondral proliferation in the synovium. The degree of ossification determines the imaging findings on plain radiographs and MR images. Ossification of the loose bodies occurs in 70 % cases and is termed *synovial osteochondromatosis. Synovial chondromatosis,* which contains purely unmineralized cartilage, accounts for the remaining 30 %. In case of synovial osteochondromatosis, plain radiographs (Fig. 31.23) or CT scans (Fig. 31.23) demonstrate multiple even-sized calcified nodules over the joint. MR imaging demonstrates multiple even-sized intra-articular loose bodies with cartilage signal (isointense T1 and high T2 signal intensity). Areas of dark T1 and T2 signal within the individual loose bodies are seen in cases of ossification and are more conspicuous on gradient echo sequences due to blooming. With maturation of bone cortex in the loose bodies, mature fatty marrow signal (high T1 and high T2 signal) can be detected on MR.

31.4.3.3 Lipoma Arborescens

Lipoma arborescens is a benign fatty proliferative disease of the synovium that is rare in children. The knee is the most commonly affected joint. Plain radiographs demonstrate joint effusion. MR findings are characteristic with frond-like synovial proliferation with persistent fat signal on all sequences (Fig. 31.24) (Martin et al. 1998; Vilanova et al. 2003). While lipoma arborescens is commonly associated with degenerative joint disease in adults, it can occur in a younger population without underlying disease.

31.4.3.4 Childhood Malignancies Presenting with Arthritis

Some childhood malignancies can present with arthritis clinically mimicking inflammatory arthritis, including metastatic neuroblastoma (Fig. 31.25), lymphoma, leukemia (Fig. 31.26), and primary bone tumors. Leukemic arthritis is more common in children and is seen in 12–65 % of pediatric leukemia. It typically presents with transient joint pain with a predilection for large joints such as knees and shoulders. Leukemic infiltration of the synovium, hemorrhage, and metaphyseal periostitis cause joint pain and can be seen in the absence of hematologic abnormality in 5 % of patients. Radiologic findings include joint effusion, periostitis, lytic or sclerotic bone lesions, and metaphyseal lucent bands, although plain radiograph findings are often normal. MR imaging demonstrates diffuse abnormal bone marrow with low T1 and high T2 signal intensities (Fig. 31.26) (Cohen et al. 1984).

31.4.3.5 Synovial Vascular Malformation

Vascular malformation involvement of the intra-articular space is rare, but typically presents in children and young adults. It is classified by the type of vasculature: capillary, venous, arterial, lymphatic, and mixed components. Intra-articular synovial involvement results in recurrent hemarthrosis and can be misdiagnosed as hemophilic arthropathy. Delayed diagnosis can lead to poor clinical outcome with progressive arthropathy. Plain radiographs can demonstrate soft tissue mass, phlebolith, maturation of the epiphysis, arthropathy, and leg-length discrepancy. MR findings of vascular malformation depend on the vascular component; venous type has homogeneous enhancement (Fig. 31.27), while lymphatic type has peripheral enhancement on post-contrast images (Fig. 31.27). Arteriovenous malformations have flow voids on T2-weighted images due to the high flow nature of the vessel (Legiehn and Heran 2006).

31.5 Noninfectious Inflammatory Diseases of the Soft Tissue

31.5.1 Dermatomyositis

Juvenile dermatomyositis (JDM) is the most common type of inflammatory myopathy and typically occurs in children between 5 and 14 years of age. It is characterized by insidious onset of bilateral symmetric muscle weakness and violaceous skin rash. Skin rash and three of the following four criteria are necessary for diagnosis of JDM: proximal muscle weakness, elevated muscle enzymes, findings of inflammatory myopathy on electromyography (EMG), and/or inflammatory myositis on muscle biopsy. MR imaging shows symmetric muscle and perimuscular edema on water-sensitive sequences (T2-weighted image with fat suppression or short inversion recovery (STIR) sequences) (Fig. 31.28). Soft tissue calcification is seen in 30–70 % of patients and occurs at areas exposed to trauma (elbows, knees, and buttocks) (Fig. 31.29). MR imaging is useful to evaluate muscle edema/inflammation as well as to localize muscle biopsy. Reticulated high T2 signal changes in subcutaneous fat are associated with a more aggressive and chronic course of the disease process (Johnson et al. 2006; Ladd et al. 2011).

31.5.2 Eosinophilic Fasciitis

Eosinophilic fasciitis is a rare disease entity of diffuse fasciitis associated with serum eosinophilia. It presents with significant extremity swelling followed by skin indurations. MR imaging demonstrates high T2 signal within the fascia and fascial thickening with adjacent muscle edema and fascial enhancement on post-contrast T1-weighted images (Fig. 31.30) (Moulton et al. 2005). MR imaging is also useful to reassess patients after treatment.

31.6 Illustrations: Infection and Inflammation of the Musculoskeletal System

31.6.1 Infectious Disorder of the Bone and Joint; Acute Osteomyelitis

Fig. 31.1 *A 10-year-old boy with acute osteomyelitis.* (**a**) Plain radiograph of the right femur demonstrates no bony abnormalities. (**b**) Bone scan 2 h delayed image demonstrates increased uptake in the proximal diaphysis of the right femur (*arrows*). (**c**) Sagittal T2-weighted MR image demonstrates bone marrow edema (*) with poor interface between normal and abnormal marrow as well as soft tissue swelling (*arrowheads*). (**d**) Post-contrast axial T1-WI demonstrates contrast enhancement of the bone marrow (*) and soft tissue (*small white arrows*). Soft tissue abscess with rim enhancement and internal fluid is seen (*black arrow*)

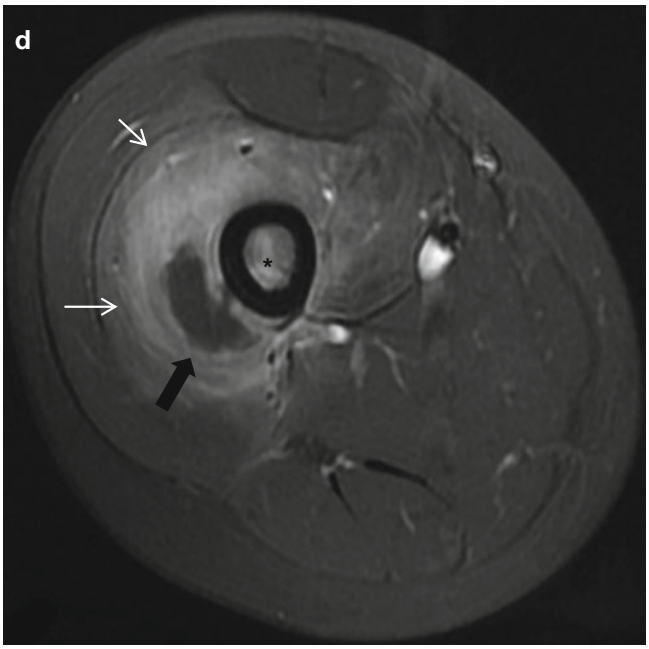

Fig. 31.1 (continued)

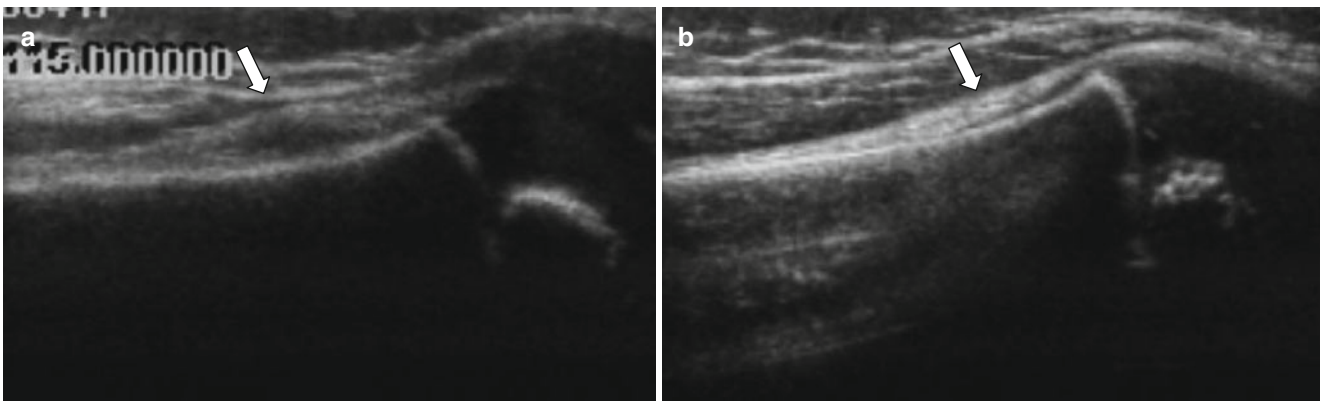

Fig. 31.2 *A 5-year-old girl with subperiosteal abscess.* (**a**) Ultrasound exam of the right femur demonstrates periosteal lifting with subperiosteal fluid (*arrow*). (**b**) Exam of the contralateral side demonstrates normal appearance of the periosteum (*arrow*)

Fig. 31.3 *A 12-year-old girl with Brodie's abscess.* (**a**) Plain radiograph of the left femur demonstrates a single well-circumscribed osteolytic lesion with sclerosis (*arrows*). (**b**, **c**) Coronal T2-WI with fat suppression (**b**) and post-contrast sagittal T1-WI with fat suppression (**c**) demonstrate an area of fluid signal (*) with enhancing rim (*black arrows*). Subperiosteal abscess is seen (*white arrow*)

Fig. 31.4 *A 3-month-old boy with sclerosing osteomyelitis. Subacute-chronic phase:* 2 months after disease onset. (**a**) Plain radiographs of the right tibia-fibula demonstrate cortical thickening, periosteal new bone formation (*small black arrows*), and intramedullary mixed sclerotic and osteolytic changes. Pathologic fracture is identified. *Acute phase*: immediately (6 days) after disease onset. (**b**) Plain radiograph demonstrates soft tissue swelling (*arrowheads*). (**c**) Post-contrast T1-WI MR image demonstrates soft tissue swelling, bone marrow enhancement, and subperiosteal abscess formation (*arrow*)

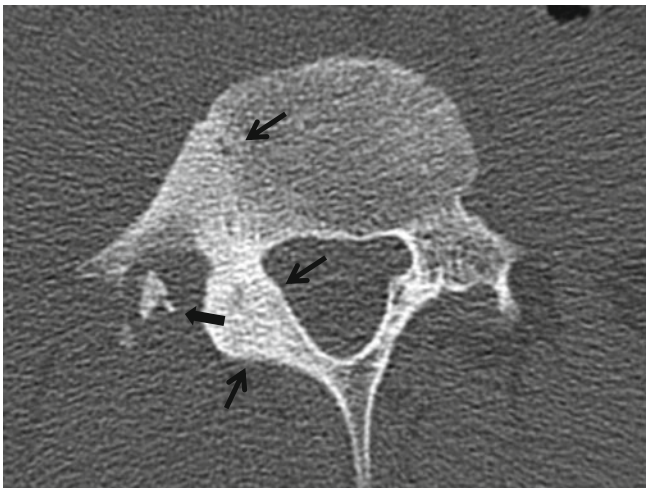

Fig. 31.5 *A* 16*-year-old boy with sequestrum of the lumbar spine.* CT scan of the lumbar spine demonstrates sequestrum (*arrow*) surrounded by soft tissue. Right transverse process and posterior element of the spine show cortical thickening and sclerosis (*small black arrows*)

31.6.2 Infectious Disorder of the Bone and Joint; Septic Arthritis

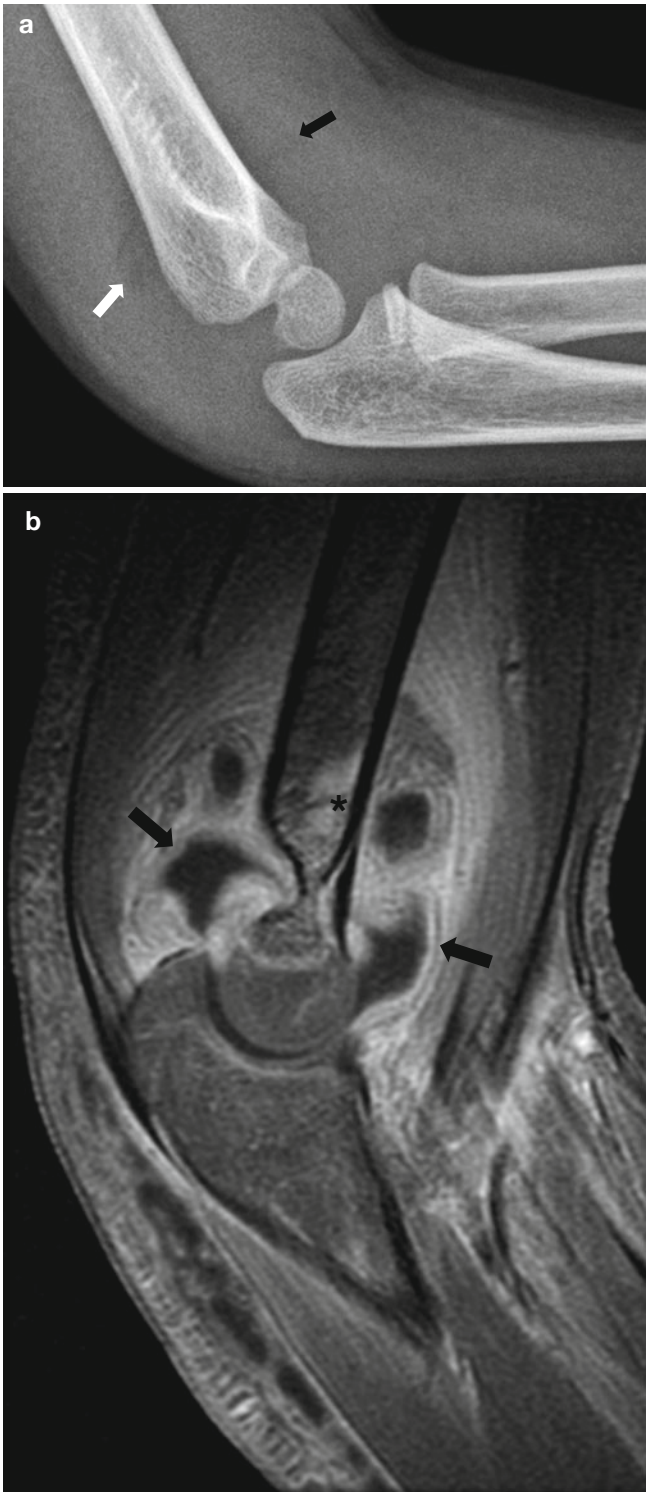

Fig. 31.6 *A 3-year-old girl with septic arthritis.* (**a**) Plain radiograph of the elbow demonstrates a large joint effusion with shifting of the anterior (*black arrow*) and posterior (*white arrow*) fat pads. (**b**) Post-contrast sagittal T1-WI with fat suppression demonstrates abundant enhancing synovium (*black arrows*), soft tissue swelling, and bone marrow edema (*)

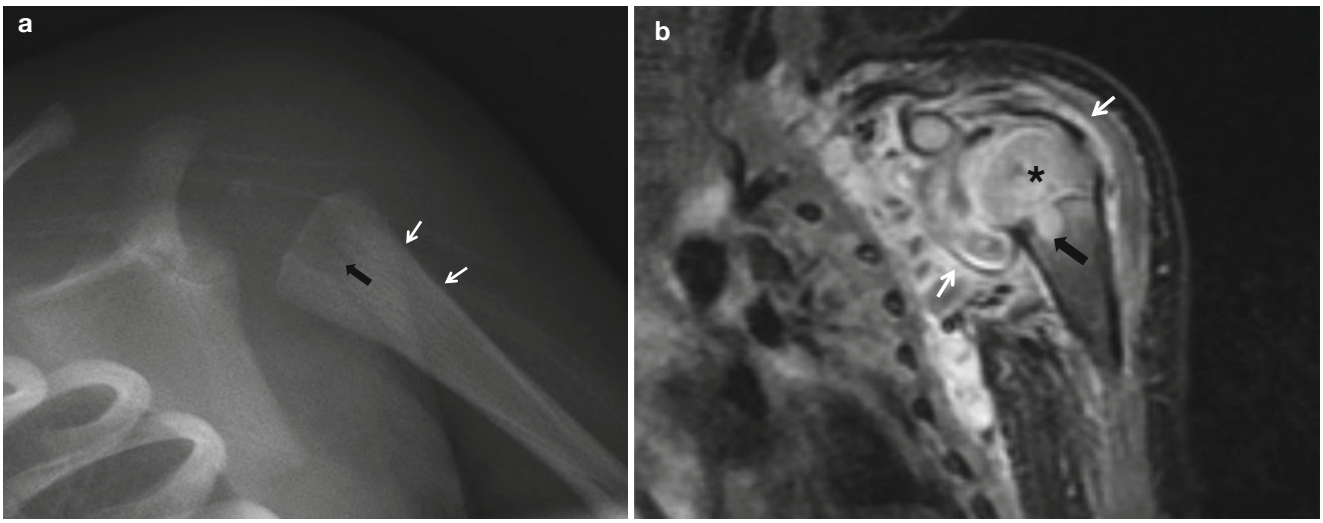

Fig. 31.7 *A 3-week-old girl with septic arthritis.* (**a**) Plain radiograph of the left shoulder demonstrates periosteal reaction (*small white arrows*) and destructive change (*black arrow*) of the left proximal humerus. (**b**) Post-contrast coronal T1-WI with fat suppression demonstrates synovial enhancement (*small white arrows*) and intraosseous abscess formation (*black arrow*). Bone marrow edema and enhancement of the epiphysis of the humerus suggesting osteomyelitis is seen (*)

31.6.3 Infectious Disorder of the Bone and Joint; Tuberculous Arthritis

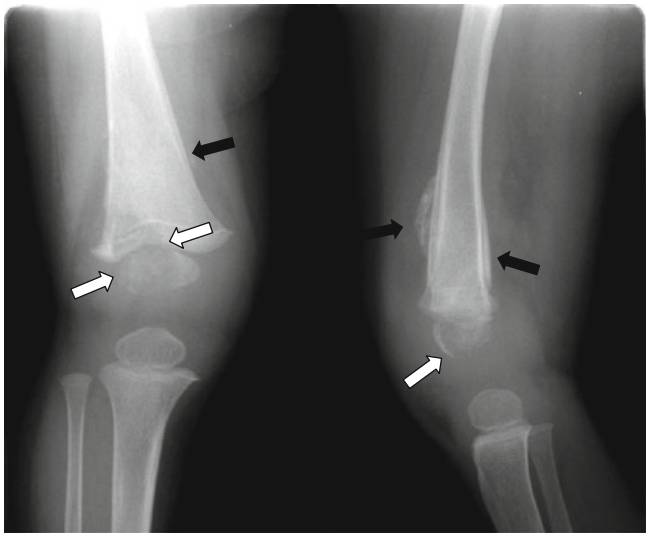

Fig. 31.8 *A 2-year-old girl with tuberculosis.* Plain radiograph of the right distal femur demonstrates bone destruction (*white arrows*) and periosteal reaction (*black arrows*) (Courtesy of JE Cheon M.D., Seoul, Korea)

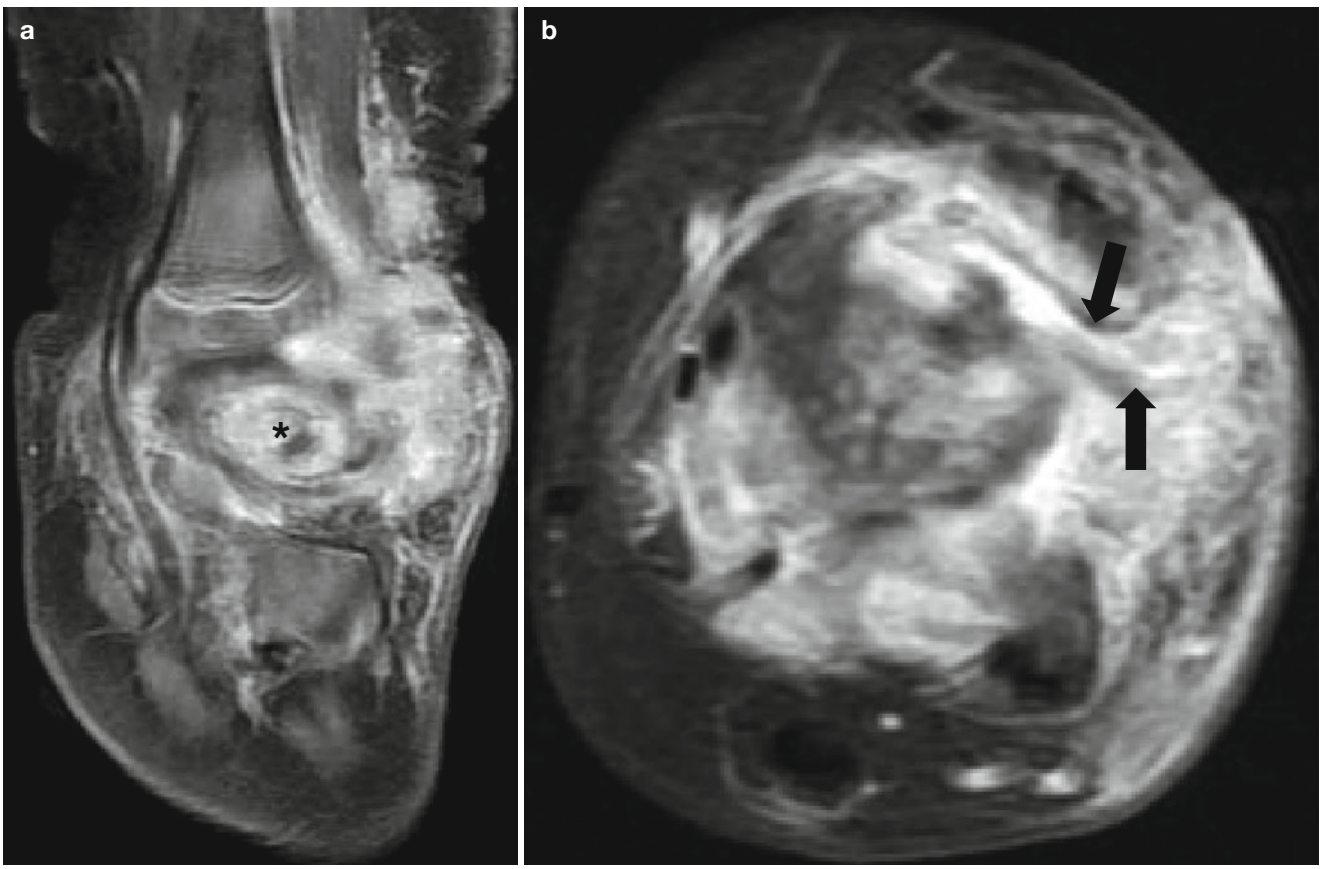

Fig. 31.9 *A 2-year-old girl with tuberculosis arthritis of the ankle.* (**a**) Post-contrast sagittal T1-WI with fat suppression demonstrates intraosseous abscess formation and bone erosion (*) and synovitis. (**b**) Post-contrast axial T1-WI with fat suppression demonstrates dermal sinus track with tram track appearance (*arrows*) (Courtesy of JE Cheon M.D., Seoul, Korea)

31.6.4 Infectious Disorder of the Bone and Joint; Congenital Syphilis

Fig. 31.10 *Congenital syphilis.* (**a**) Infantogram of a newborn baby demonstrates multifocal metaphyseal lucent bands (*arrows*). (**b**, **c**) A 2-month-old boy with congenital syphilis. Radiographs of the wrist (**b**) and lower leg (**c**) demonstrate metaphyseal lucencies (*black arrow*) and multiple areas of periosteal new bone formation (*white arrows*). (**d**) Another 2-month-old boy with congenital syphilis. Lower extremity and cone-down view of the right knee show Wimberger's sign bilaterally (*black arrows*). Characteristic Laval-Jeantet collar, representing spared newly formed metaphysis, is seen (*white arrow*)

31.6.5 Infectious Disorders of the Soft Tissue; Pyomyositis

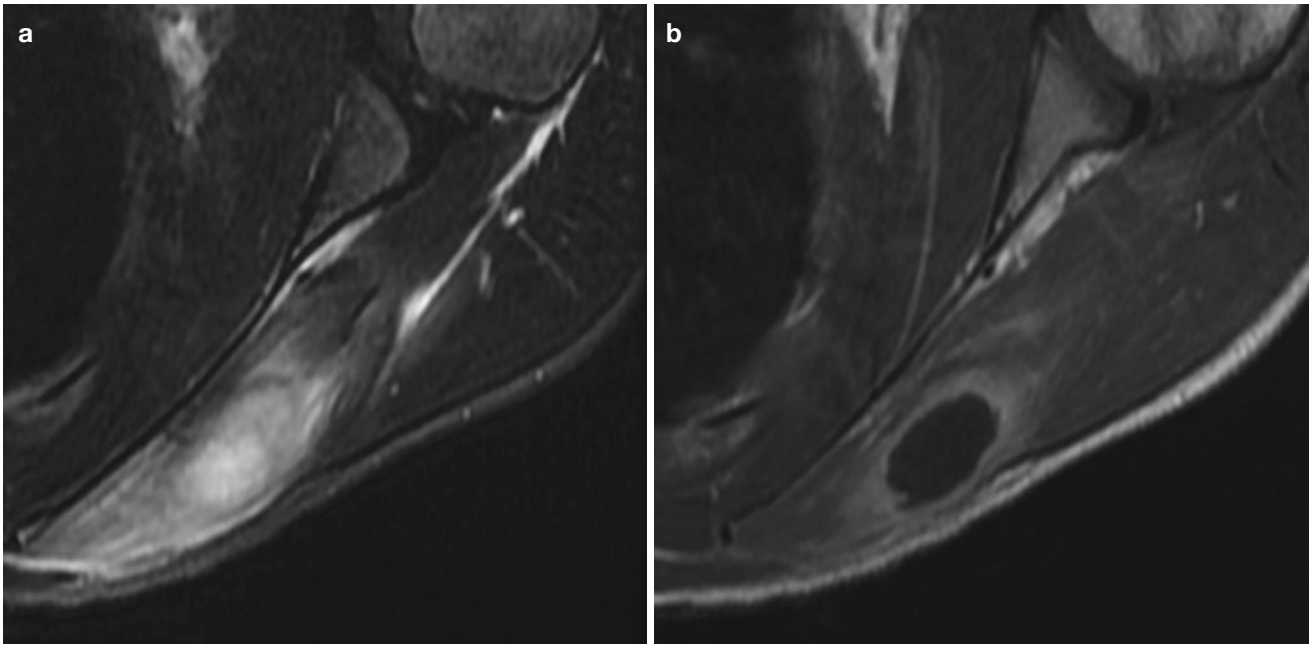

Fig. 31.11 *A* 11*-year-old boy with pyomyositis of the shoulder*. (**a**) Axial T2-WI with fat suppression and (**b**) Post-contrast axial T1-WI with fat suppression demonstrate well-circumscribed fluid collection with rim enhancement

31.6.6 Noninfectious Inflammatory Diseases of the Bones and Joints; Juvenile Idiopathic Arthritis

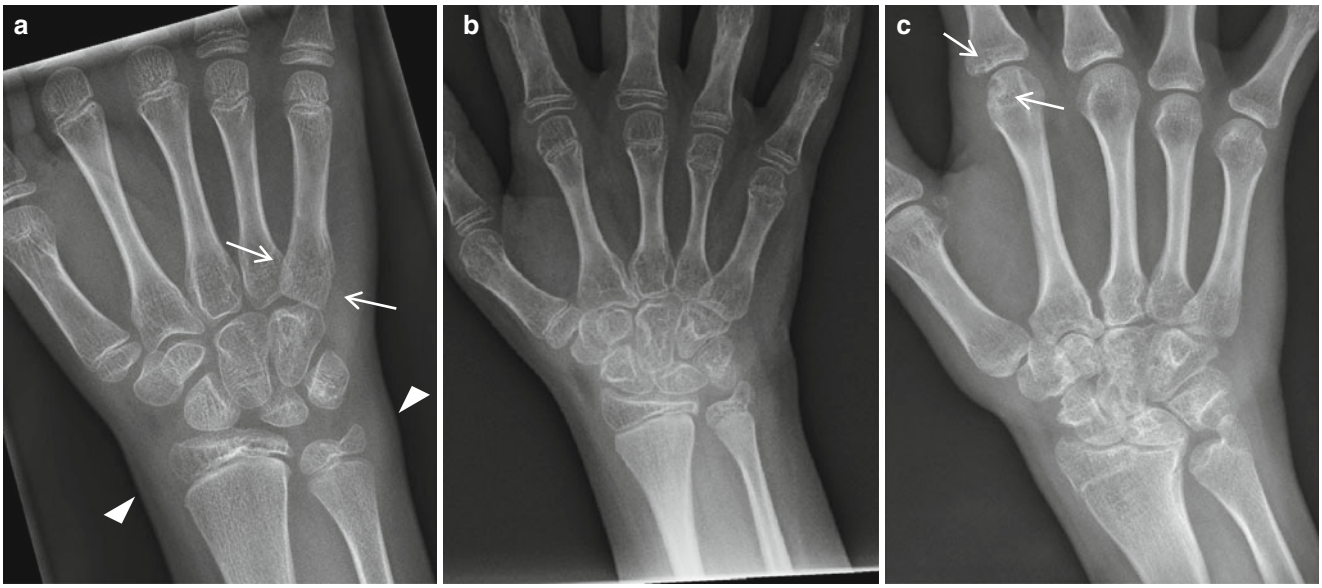

Fig. 31.12 *Juvenile idiopathic arthritis in different stages in different patients.* (**a**) A 9-year-old girl with JIA. Wrist radiograph demonstrates periarticular osteopenia (*white arrows*) and soft tissue swelling (*arrow heads*). (**b**) An 11-year-old girl with JIA. Wrist radiograph demonstrates squaring of carpal bones with intercarpal joint space narrowing. (**c**) A 15-year-old girl with JIA. Wrist radiograph demonstrates loss of joint space in the intercarpal joints due to destruction of the cartilage, proximal migration of the scaphoid and lunate bones, and erosions (*white arrows*)

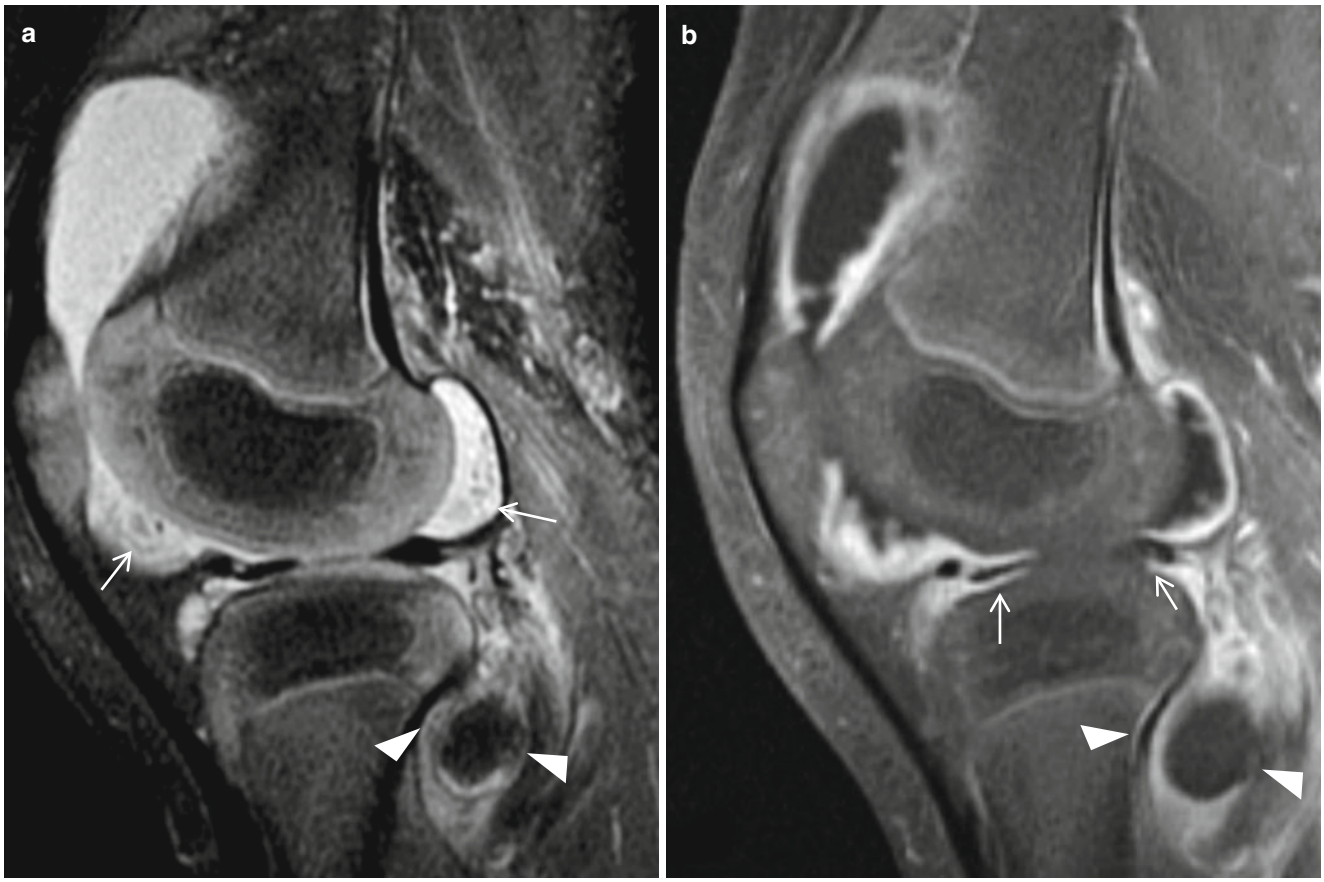

Fig. 31.13 *A 3-year-old girl with JIA.* (**a**) Sagittal T2-WI with fat suppression demonstrates a large joint effusion with high T2 signal synovium, which was not differentiated from adjacent fluid. Hypointense rice bodies (*arrows*) and popliteal cyst (*arrowheads*) are seen. (**b**) Post-contrast sagittal T1-WI with fat suppression image demonstrates diffuse synovial enhancement and popliteal cyst (*arrowheads*). Anterior and posterior horn of the meniscus is hypoplastic (*arrows*)

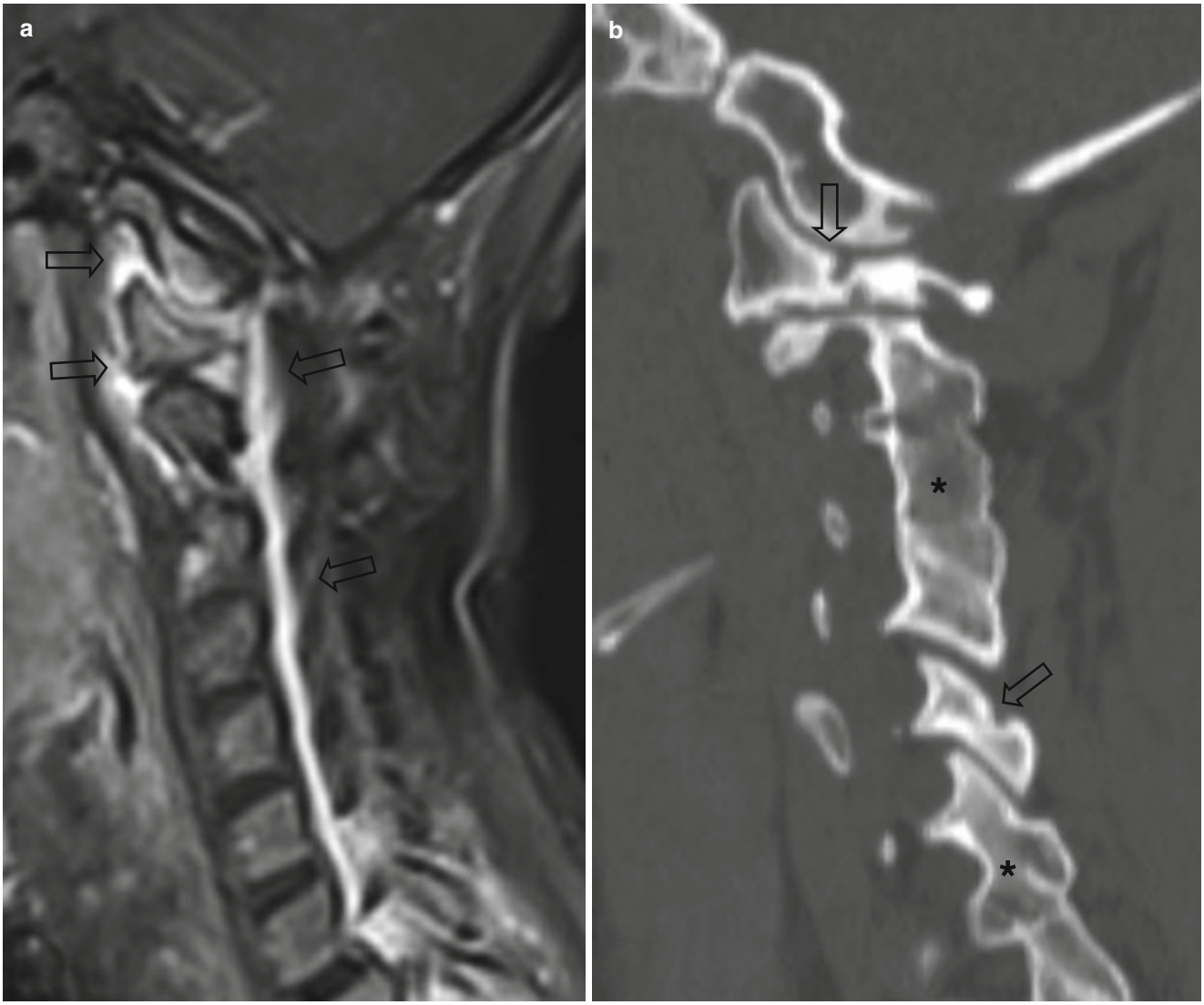

Fig. 31.14 *JIA of the cervical spine.* (**a**) A 15-year-old girl with JIA. Post-contrast sagittal T1-WI with fat suppression of the cervical spine demonstrates synovial enhancement and soft tissue swelling (*arrows*). (**b**) A 16-year-old girl with JIA. Cervical spine CT scan demonstrates bone erosion (*arrows*) and multilevel fusion of the posterior elements (*) (Courtesy of AC Merrow, M.D., Cincinnati, Ohio, USA)

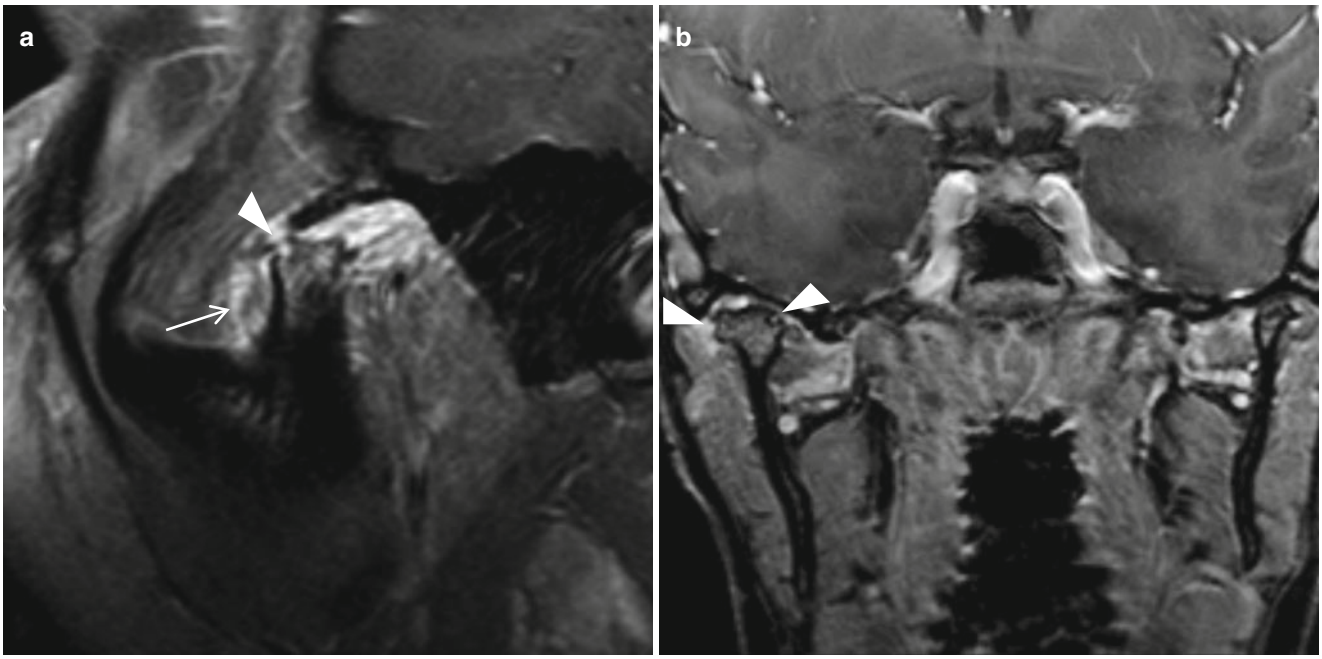

Fig. 31.15 *A 17-year-old girl with JIA of the temporomandibular joint.* (**a**) Post-contrast sagittal T1-WI with fat suppression with the patient open mouth demonstrates dislocation of the mandibular condyle, synovial enhancement (*arrow*), and flattening and shortening of the mandibular condyle with erosion (*arrowhead*). (**b**) Coronal post-contrast T1-WI with fat suppression with the patient closed mouth demonstrates both mandibular condyles are within the joints. Hypertrophy of the right mandibular condyle with flattening and erosion (*arrowhead*) is seen

31.6.7 Noninfectious Inflammatory Diseases of the Bones and Joints; Juvenile Spondyloarthropathies

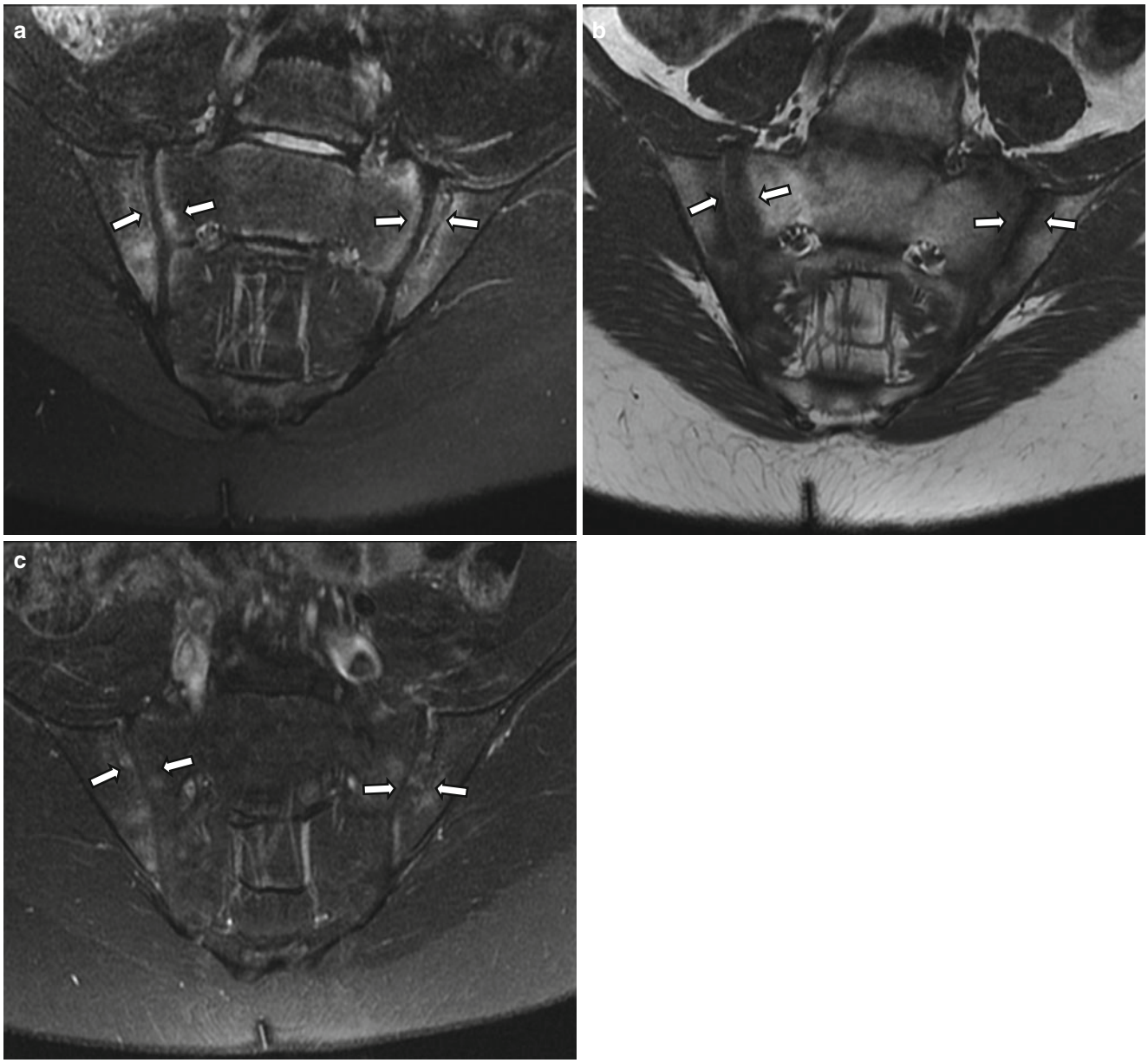

Fig. 31.16 *A* 14-year-old HLA B27-positive boy with ankylosing spondylitis. Oblique coronal T2-WI with fat suppression (**a**), T1-WI (**b**), and post-contrast T1-WI with fat suppression (**c**) demonstrate bilateral bone marrow edema (*arrows*) within the sacroiliac joint

31.6.8 Noninfectious Inflammatory Diseases of the Bones and Joints; Chronic Recurrent Multifocal Osteomyelitis

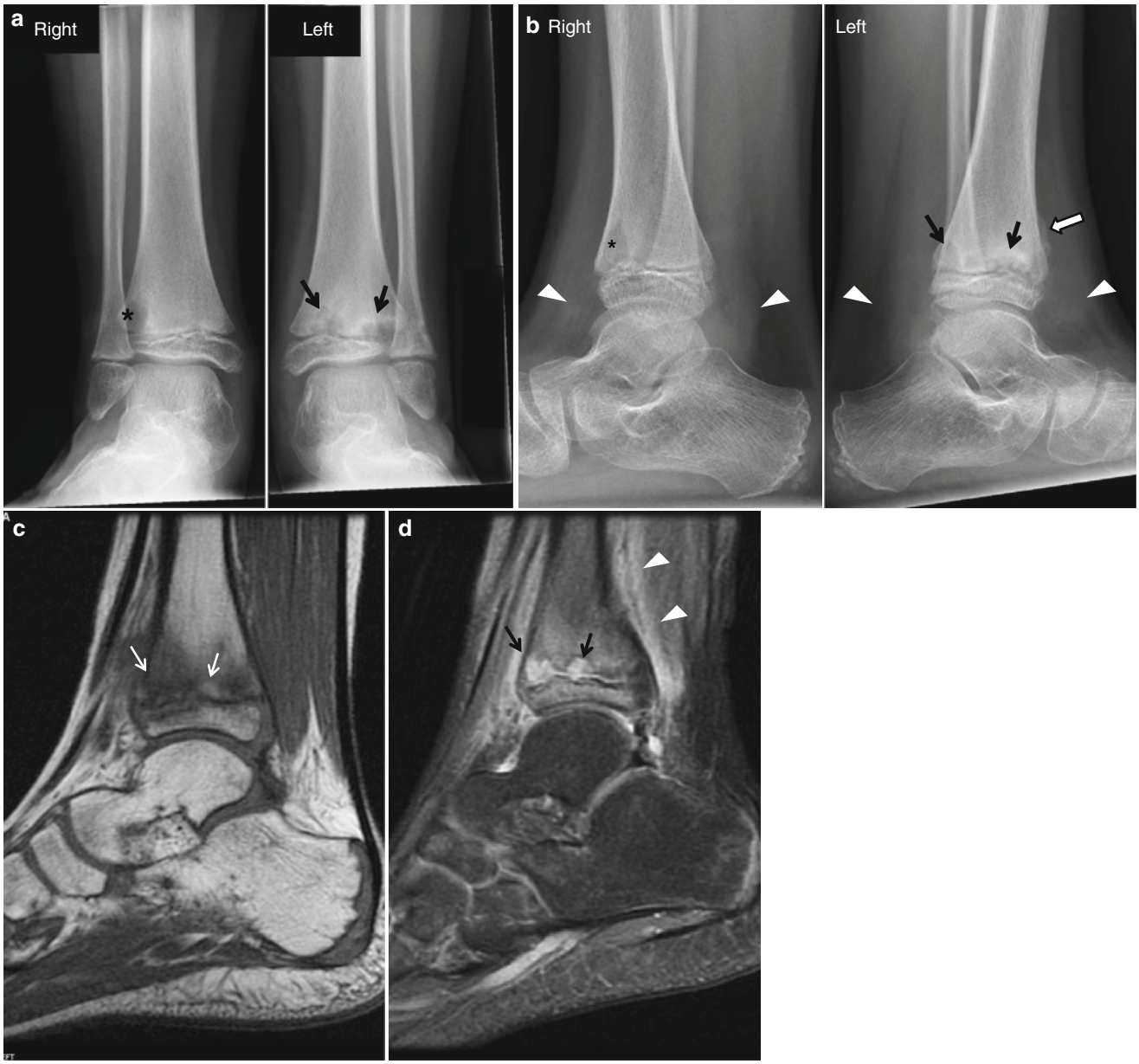

Fig. 31.17 *A 14-year-old boy with chronic recurrent multifocal osteomyelitis (CRMO).* (**a**) Frontal radiographs of the ankles demonstrate an osteolytic lesion (*) on the right and metaphyseal sclerosis and lucencies (*arrows*) on the left. (**b**) Lateral radiographs demonstrate deep soft tissue swelling (*arrowheads*), an osteolytic lesion (*), metaphyseal sclerosis and lucencies (*arrows*), and periosteal reaction (*white arrow*). (**c**, **d**) Sagittal T1-WI (**c**) and T2-WI with fat suppression (**d**) of the left ankle demonstrate a well-circumscribed area of low T1 and high T2 signal of the metaphysis (*arrows*) and soft tissue swelling (*arrowheads*)

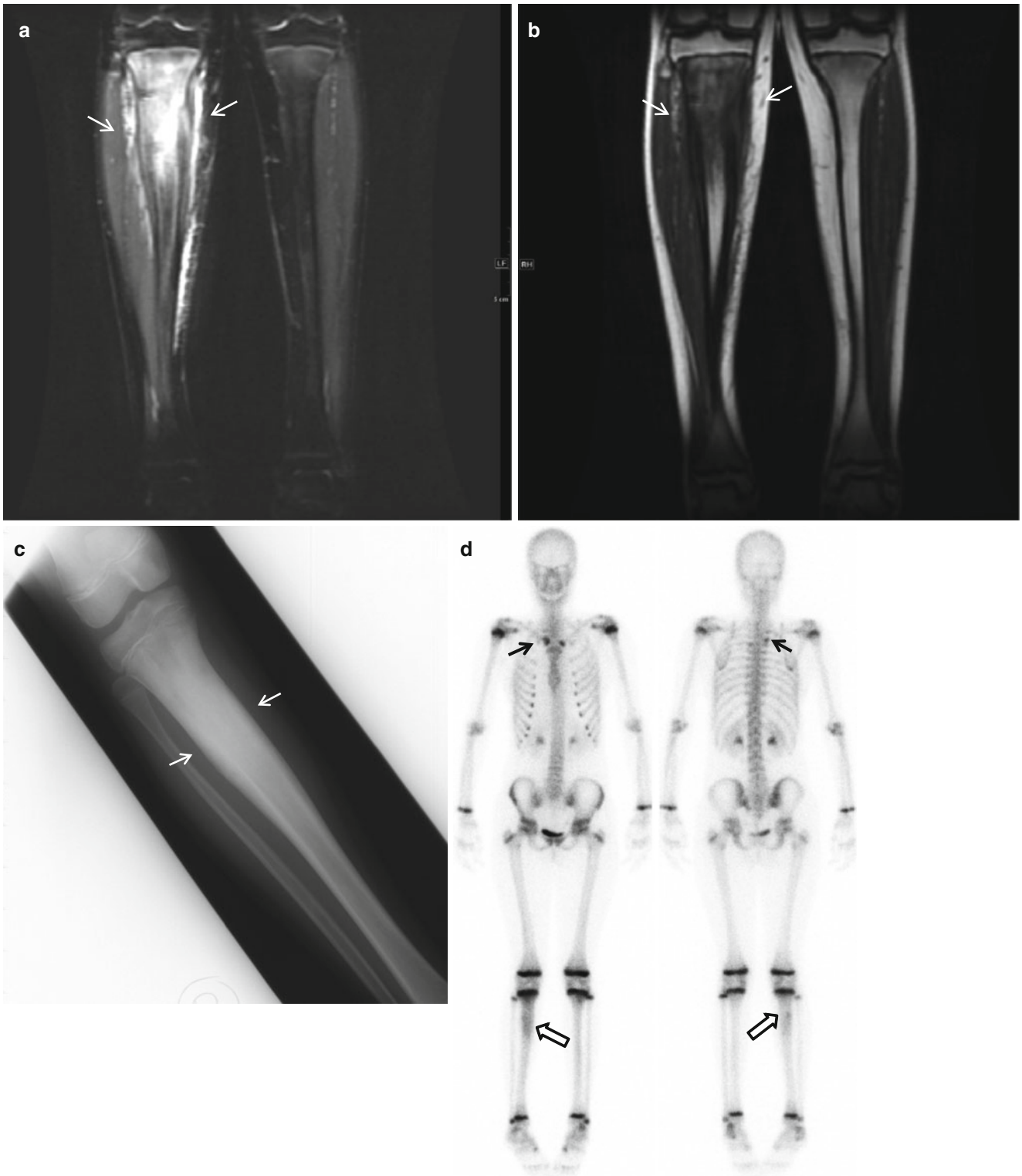

Fig. 31.18 *A 12-year-old girl with CRMO.* (**a**, **b**) Coronal T2-WI with fat suppression (**a**) and T1-WI (**b**) demonstrate bone marrow edema with soft tissue swelling (*arrows*) of the right proximal tibial metaphysis, diaphysis, and metadiaphysis. (**c**) Follow-up radiograph 2 years after disease onset demonstrates diffuse sclerotic change and cortical thickening of the proximal tibial metadiaphysis and diaphysis (*arrows*). (**d**) Bone scan performed after the patient presented with recurrent pain in the right tibia and new onset right clavicle pain demonstrates increased uptake in the right clavicle (*small black arrows*) and right proximal tibia (*white arrows*)

31.6.9 Other Noninfectious Inflammatory Joint diseases; Hemophilic Arthropathy

Fig. 31.19 *A 17-year-old boy with hemophilic arthropathy.* (**a**) Frontal and lateral radiographs of the elbow demonstrate hypertrophy of the radial head (*arrows*), joint space narrowing, subchondral sclerosis, and cystic changes. (**b**, **c**) Sagittal T2-WI with fat suppression (**b**) and gradient echo sequence images (**c**) demonstrate linear dark signal along the synovium (*arrows*) suggesting hemosiderin deposition, subchondral cyst (*arrowhead*), and joint space narrowing

31.6.10 Other Noninfectious Inflammatory Joint Diseases; Neuropathic Arthritis

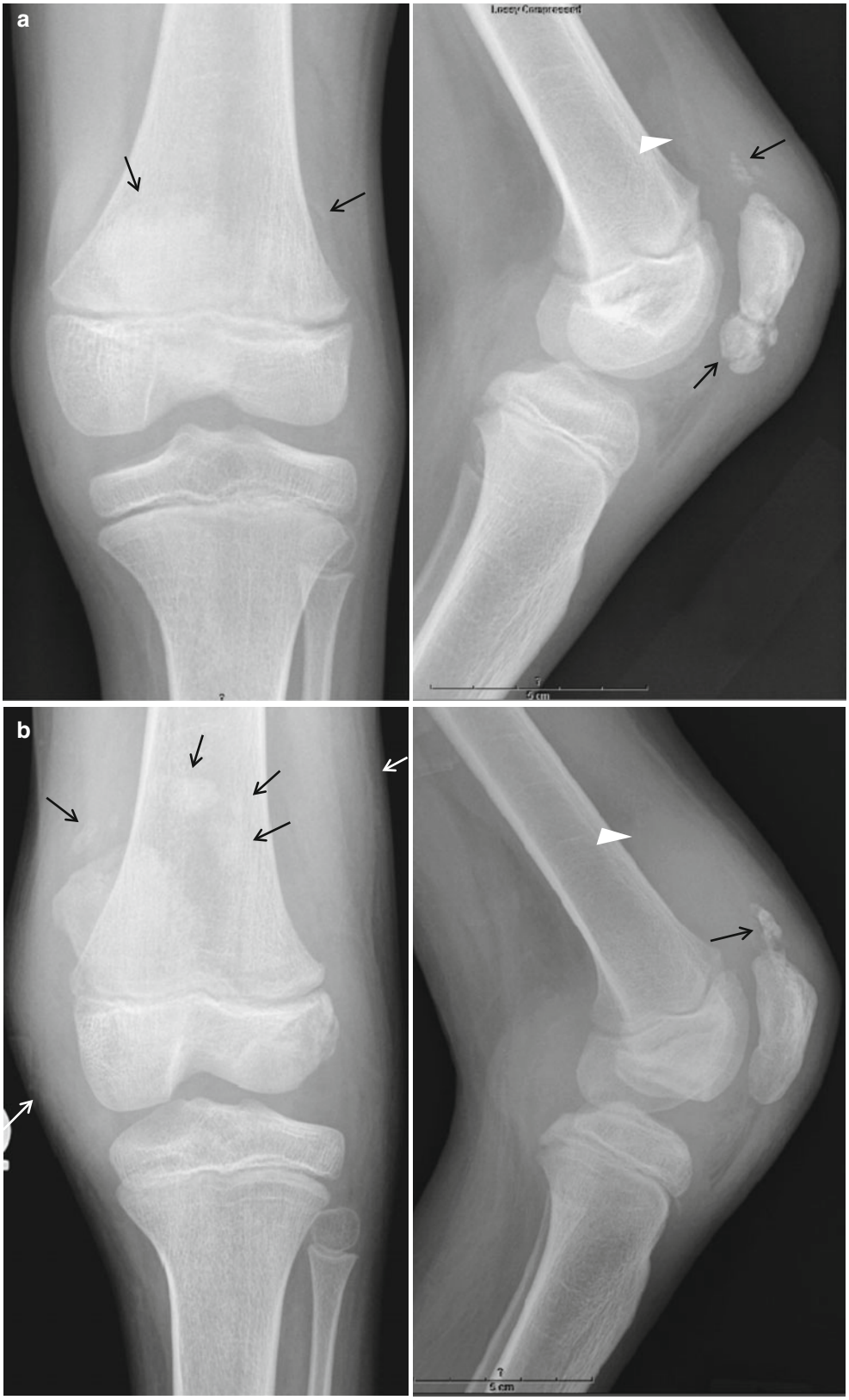

Fig. 31.20 *A 6-year-old boy with myelomeningocele and neuropathic joint.* (**a**) Initial radiographs of the knee joint demonstrate fragmentation of the patella (*arrows*) and a large joint effusion (*arrowhead*). (**b**) Follow-up radiographs 8 months later demonstrate soft tissue swelling (*white arrows*), progressive fracture of the patella (*arrows*), and a large joint effusion (*arrowhead*). (**c**) Follow-up radiographs 12 months later demonstrate more soft tissue swelling and progressive fragmentation of the patella and a new finding of a lateral femoral condyle fracture. Several bone fragments are embedded in the soft tissue (*arrows*)

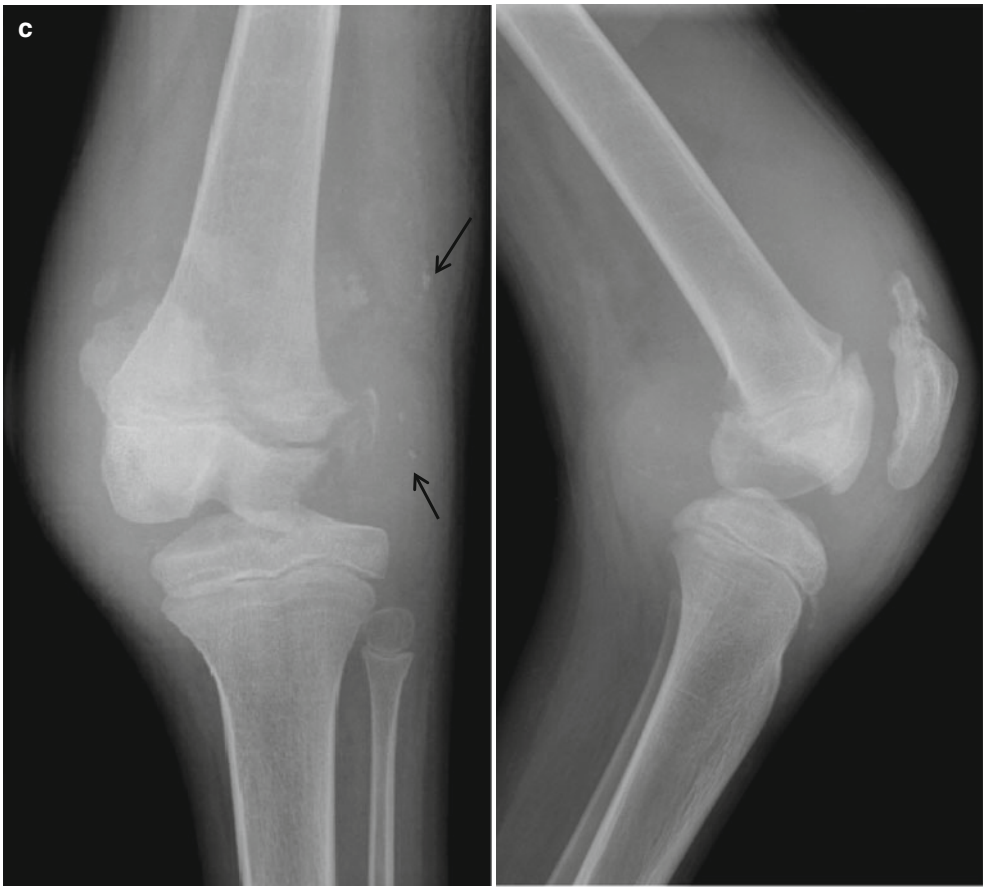

Fig. 31.20 (continued)

31.6.11 Miscellaneous Disorder of the Joint; Pigmented Villonodular Synovitis

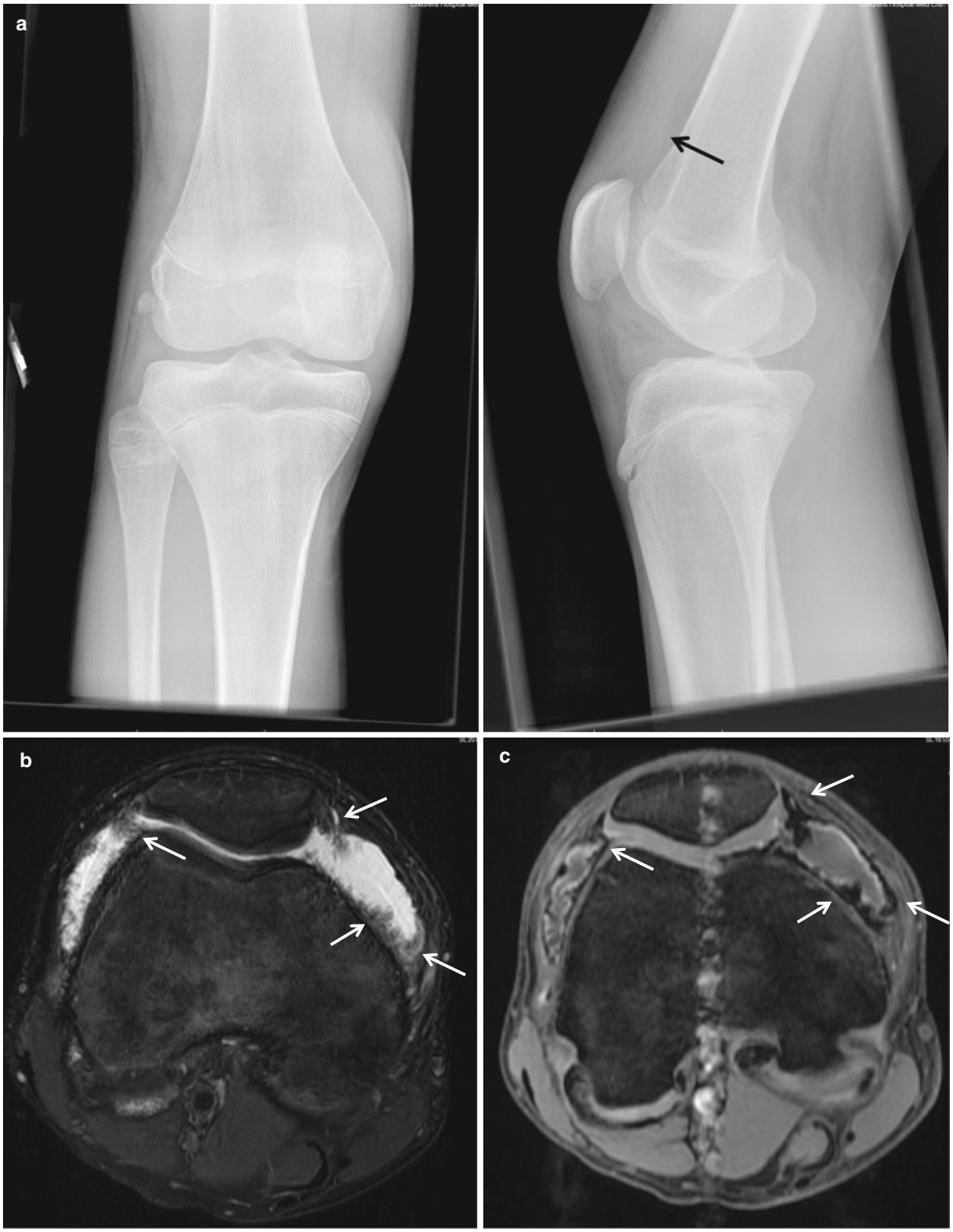

Fig. 31.21 *A 13-year-old boy with diffuse pigmented villonodular synovitis (PVNS).* (**a**) Plain radiograph demonstrates joint effusion (*arrow*). There is no bone erosion or calcification. (**b**, **c**) Axial T2-WI with fat suppression (**b**) and gradient echo sequence (**c**) demonstrate frond-like proliferation of the synovium with dark signal from hemosiderin deposition, which was more prominent on gradient echo image due to blooming artifact (*arrows*)

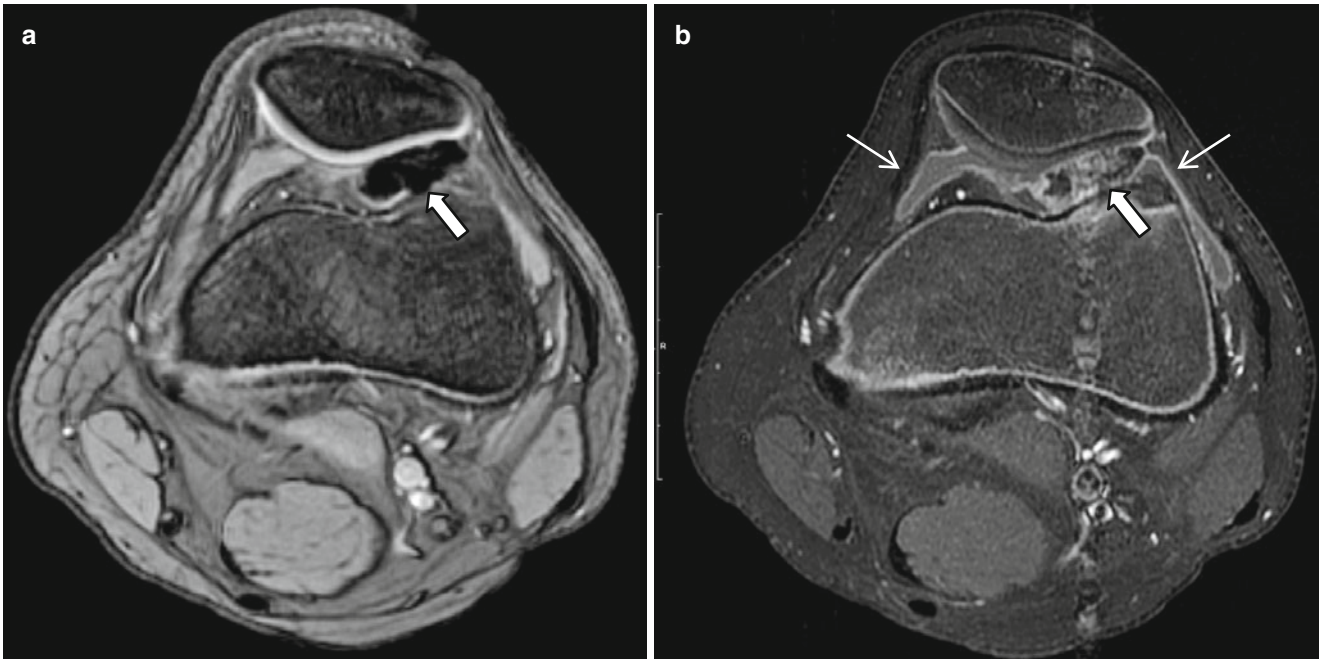

Fig. 31.22 *A 15-year-old boy with localized PVNS.* (**a**, **b**) Axial gradient echo sequence (**a**) and post-contrast axial T1-WI with fat suppression (**b**) demonstrate a single ovoid-shaped dark signal mass (*arrows*) with synovial enhancement (*small white arrows*) (Reprinted by permission from HK Kim; Pediatric Radiology. 2011:41:495–511)

31.6.12 Miscellaneous Disorder of the Joint; Synovial Osteochondromatosis

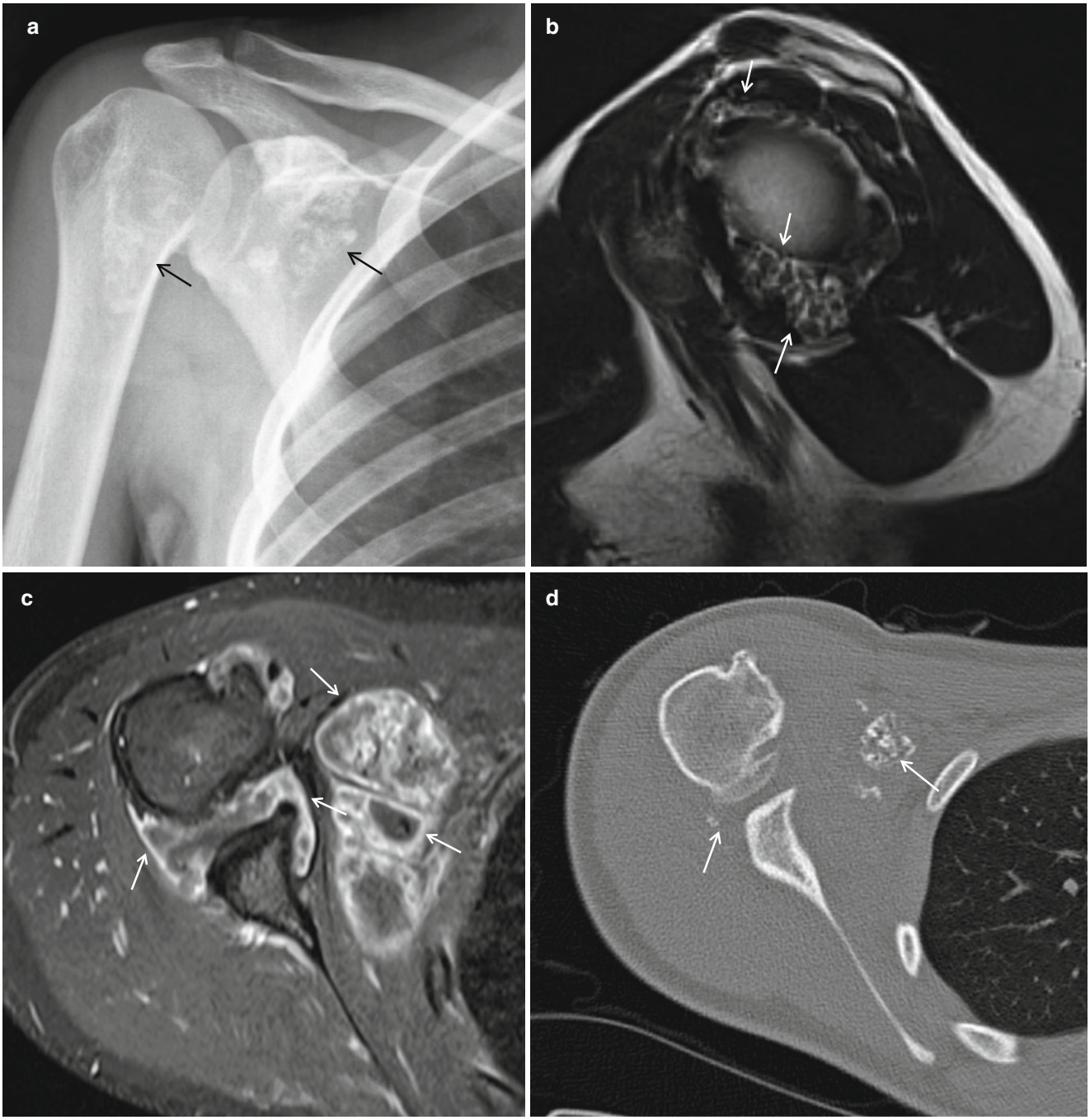

Fig. 31.23 *A 15-year-old girl with synovial osteochondromatosis.* (**a**) Plain radiograph of the shoulder demonstrates multiple calcific bodies in the right glenohumeral joint (*black arrow*). (**b**) Sagittal T2-WI demonstrates multiple dark signal even-sized intra-articular loose bodies suggesting ossified bodies. (**c**) Post-contrast axial T1-WI with fat suppression image demonstrates diffuse synovitis (*arrows*). (**d**) CT scan demonstrates even-sized calcified nodules (*arrows*) (Reprinted by permission from HK Kim; Pediatric Radiology. 2011;41:495–511)

31.6.13 Miscellaneous Disorder of the Joint; Lipoma Arborescens

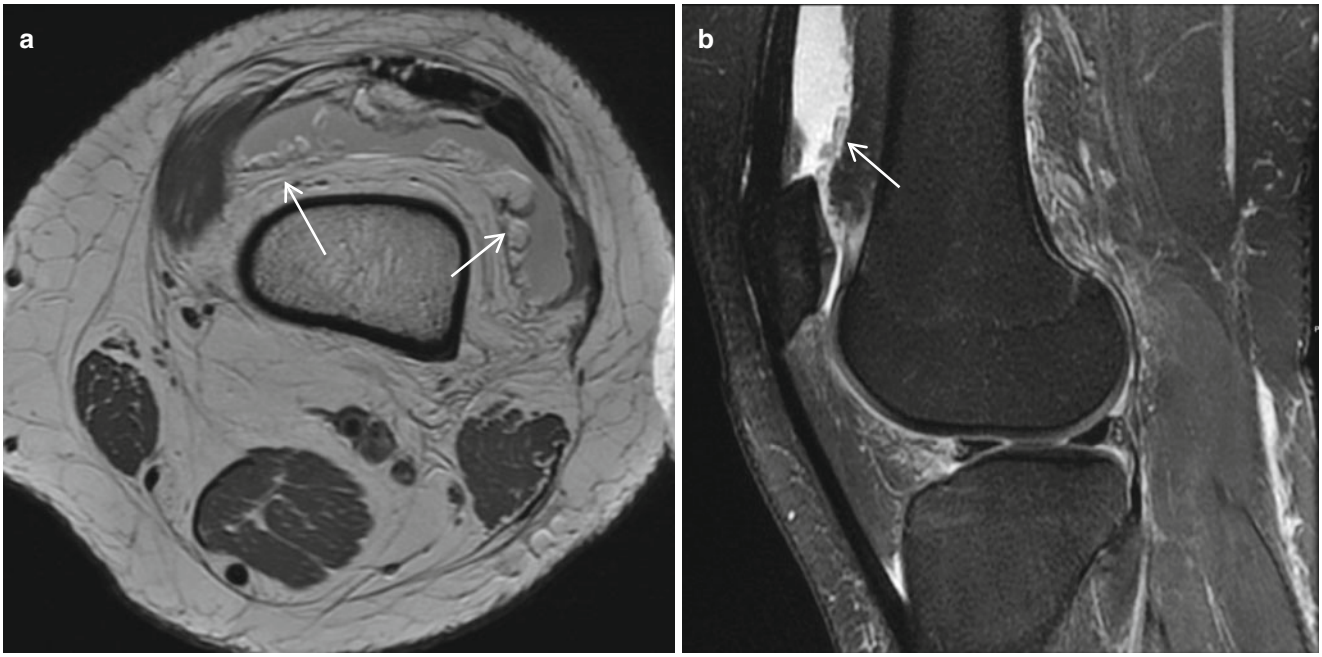

Fig. 31.24 *A 16-year-old girl with lipoma arborescens.* (**a**) Axial intermediate sequence image demonstrates frond-like fatty proliferation of the synovium (*arrows*). (**b**) Sagittal T2-WI with fat suppression demonstrates low signal intensity from fat suppression (*arrow*)

31.6.14 Miscellaneous Disorder of the Joint; Childhood Malignancies Presenting with Arthritis

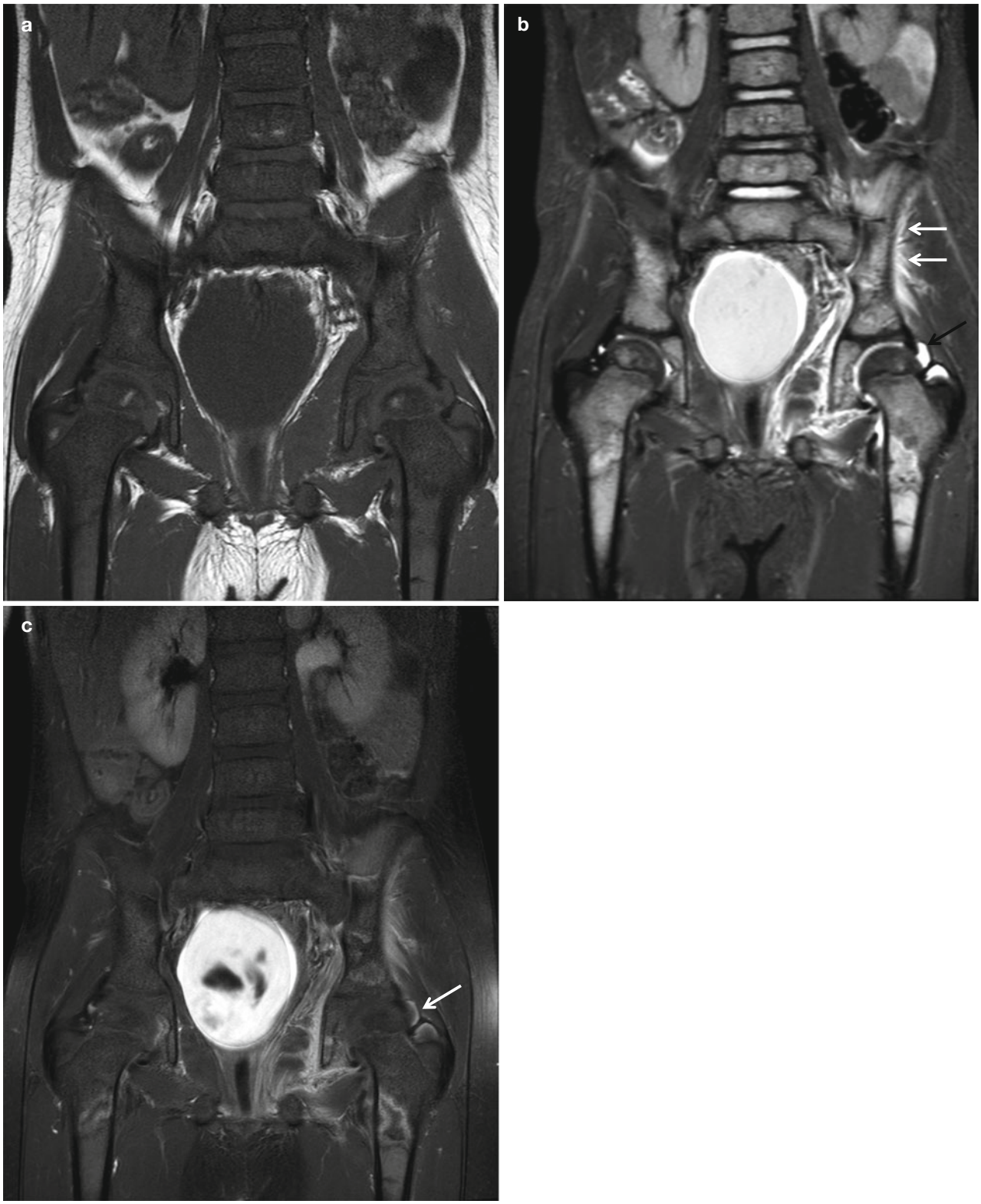

Fig. 31.25 *A 4-year-old boy with left hip pain from metastatic neuroblastoma.* (**a**, **b**) Coronal T1-WI (**a**) and T2-WI with fat suppression (**b**) demonstrate abnormal low T1 and high T2 marrow signal of the all imaged spines and pelvic bones. Left hip joint effusion (*black arrow*) and periostitis (*white arrows*) are seen. (**c**) Post-contrast coronal T1-WI with fat suppression demonstrates synovial enhancement of the left hip (*arrow*). (**d**) Metaiodobenzylguanidine (MIBG) scan demonstrates multiple sites of increased skeletal uptake suggesting bone metastasis. Metastatic neuroblastoma was confirmed by bone marrow biopsy and microscopic examination

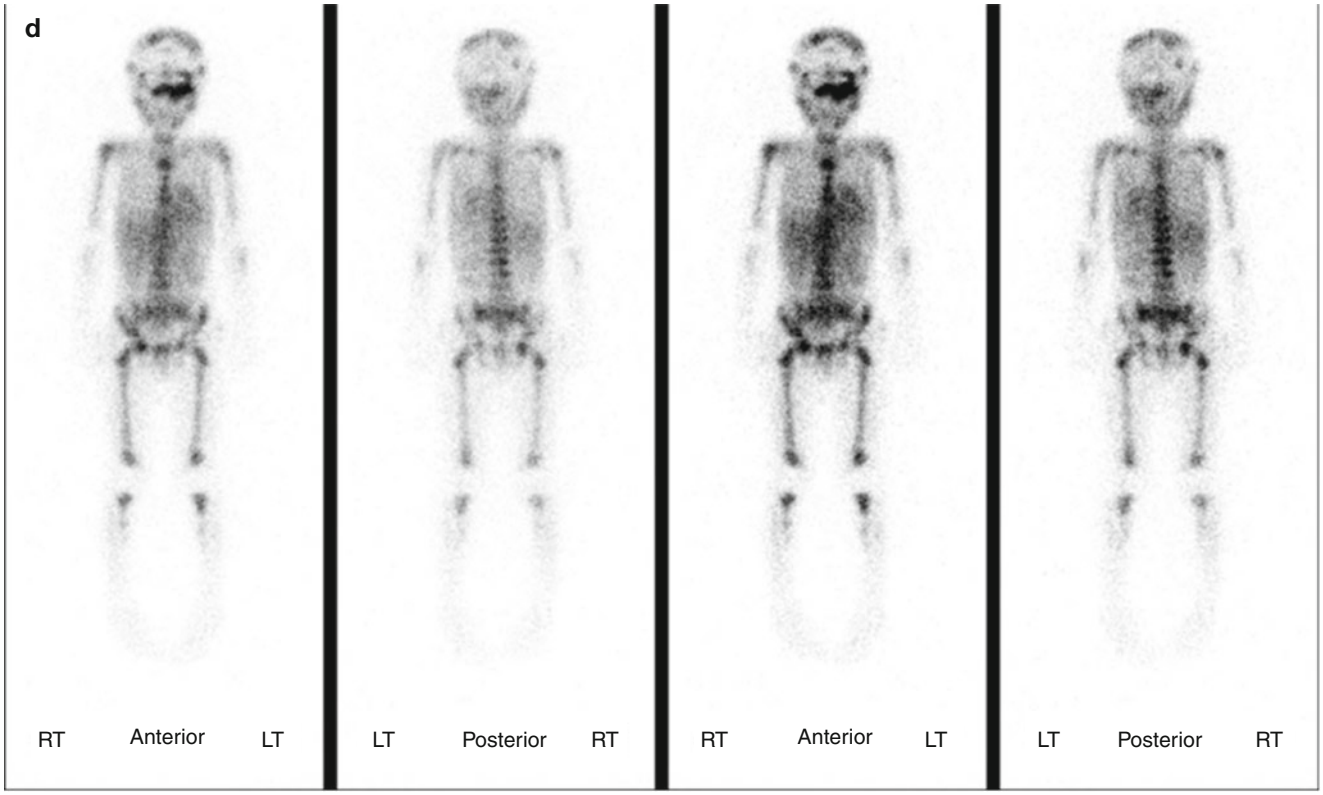

Fig. 31.25 (continued)

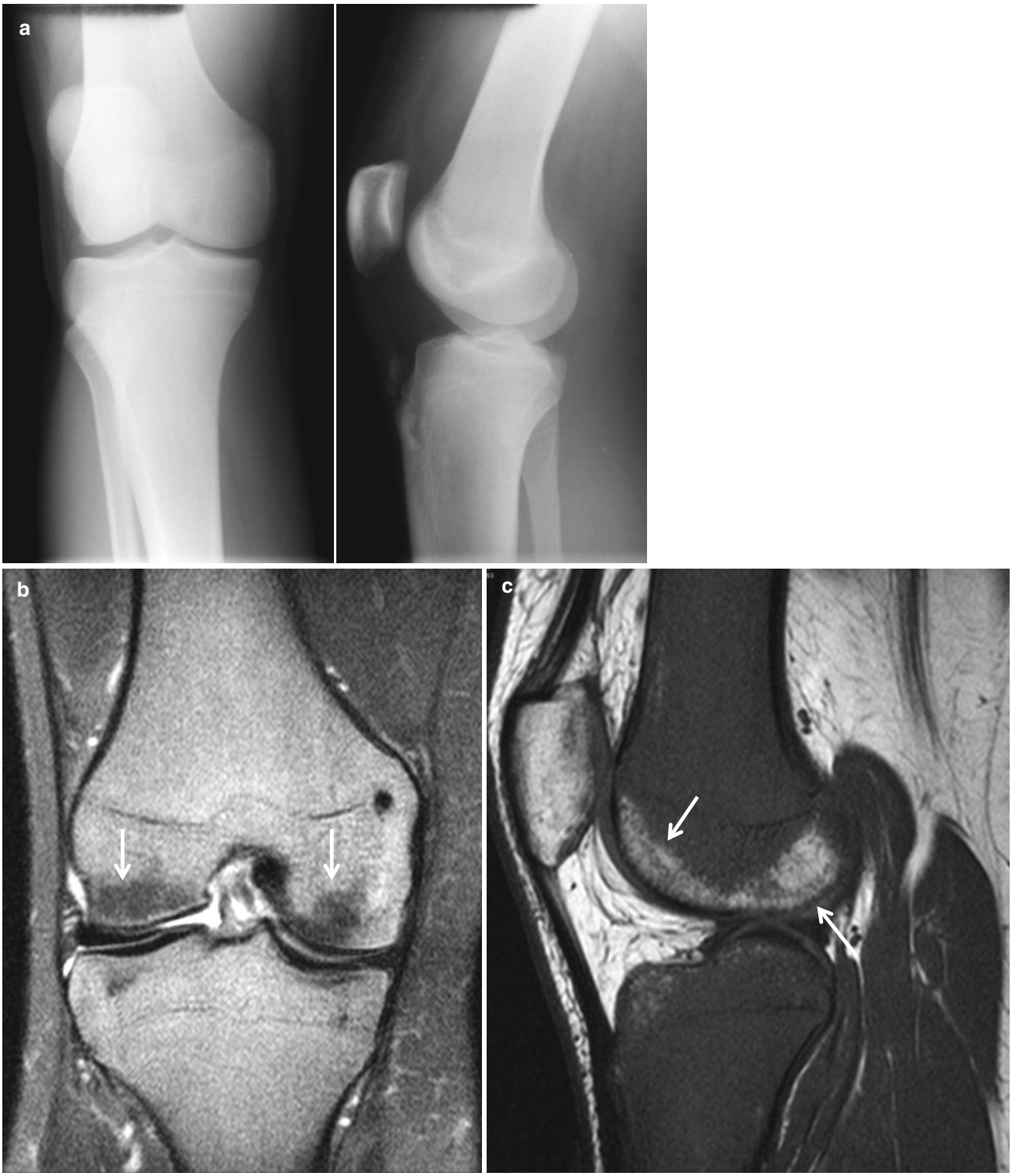

Fig. 31.26 *A 17-year-old boy presented with left knee pain from chronic myeloid leukemia.* (**a**) Plain radiographs of the knee demonstrate no bony abnormalities. (**b**, **c**) Coronal T2-WI with fat suppression (**b**) and sagittal intermediate signal intensity images (**c**) demonstrate diffuse abnormal bone marrow signal sparing the patella and a very small portion of the femoral condyles (*arrows*). Bone marrow biopsy and microscopic examination confirmed chronic myeloid leukemia

31.6.15 Miscellaneous Disorder of the Joint; Synovial Vascular Malformation

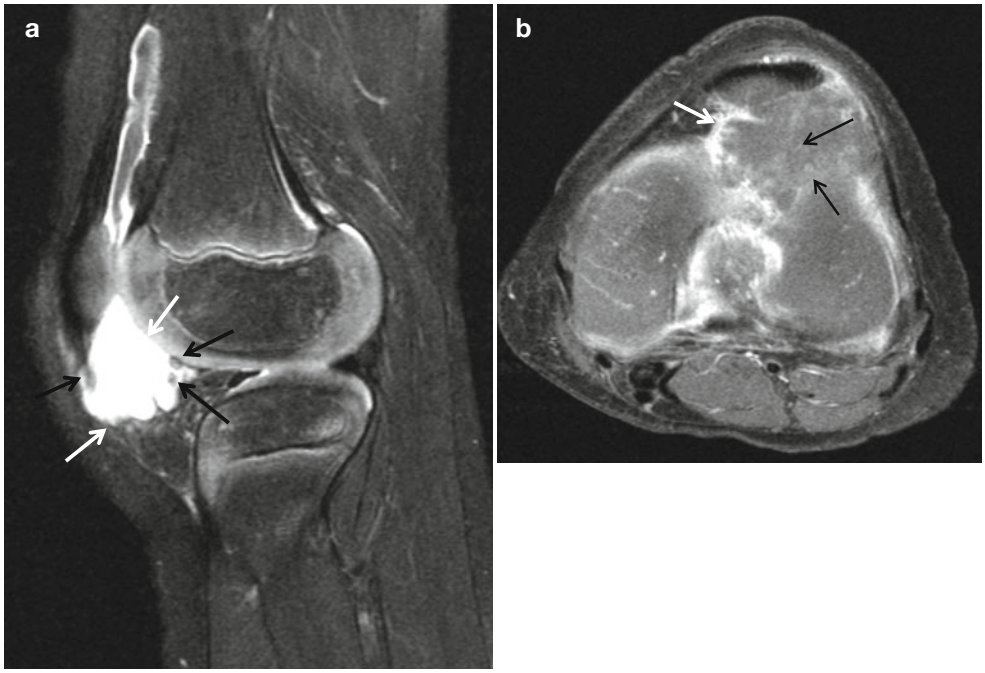

Fig. 31.27 *A 6-year-old boy with intra-articular venolymphatic malformation.* (**a**) Sagittal T2-WI with fat suppression demonstrates intra-articular high T2 signal mass (*white arrows*) with dark signal foci suggesting phleboliths (*small black arrows*). (**b**) Post-contrast axial T1-WI with fat suppression demonstrates heterogeneous enhancement suggesting a venous component and peripheral rim-like enhancement suggesting lymphatic components (*small black arrows*)

31.6.16 Noninfectious Inflammatory Diseases of the Soft Tissue; Dermatomyositis

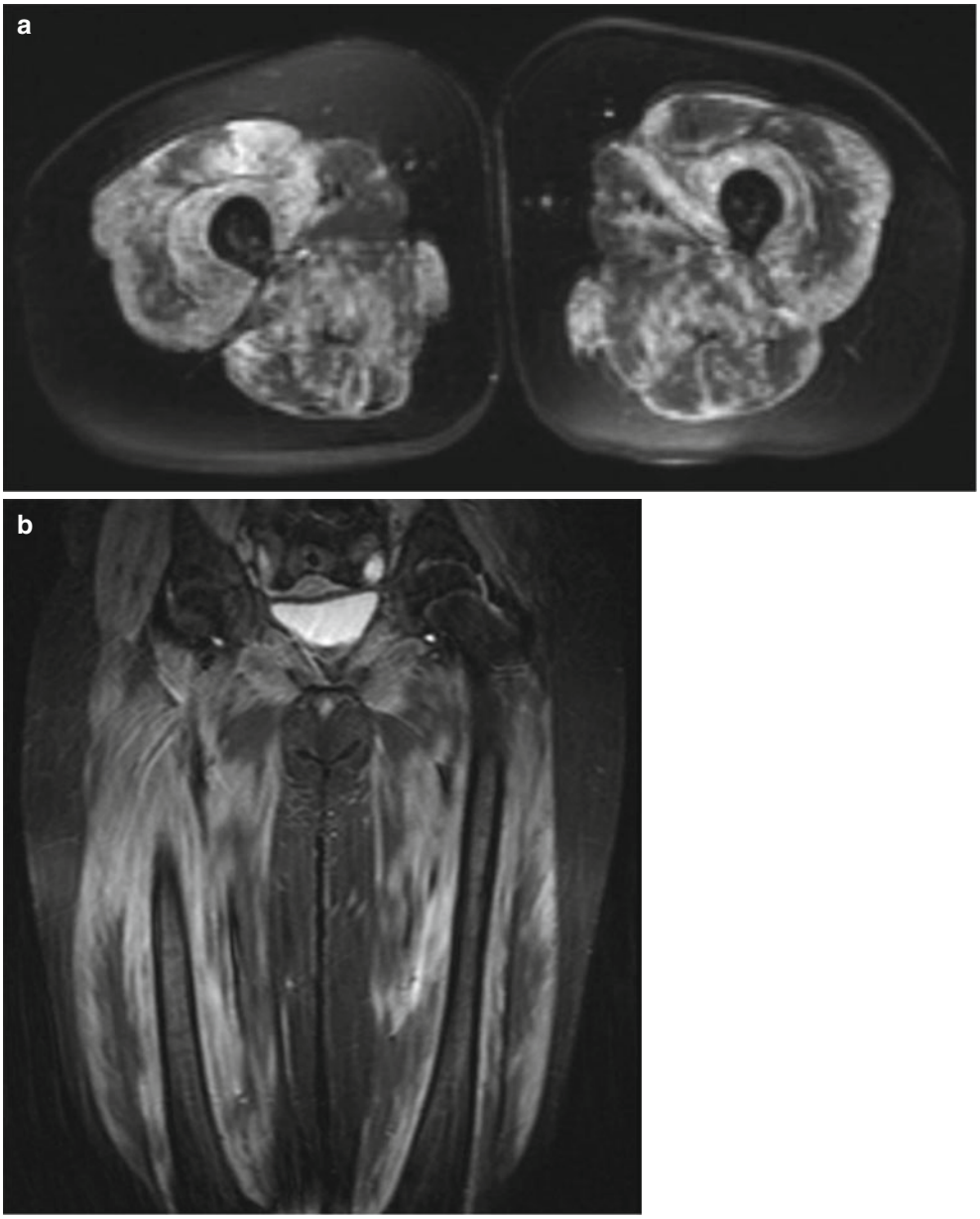

Fig. 31.28 *An* 11*-year-old girl with dermatomyositis.* (**a**, **b**) Axial (**a**) and coronal T2-WI with fat suppression images (**b**) of the thighs demonstrate bilateral muscle edema suggesting myositis

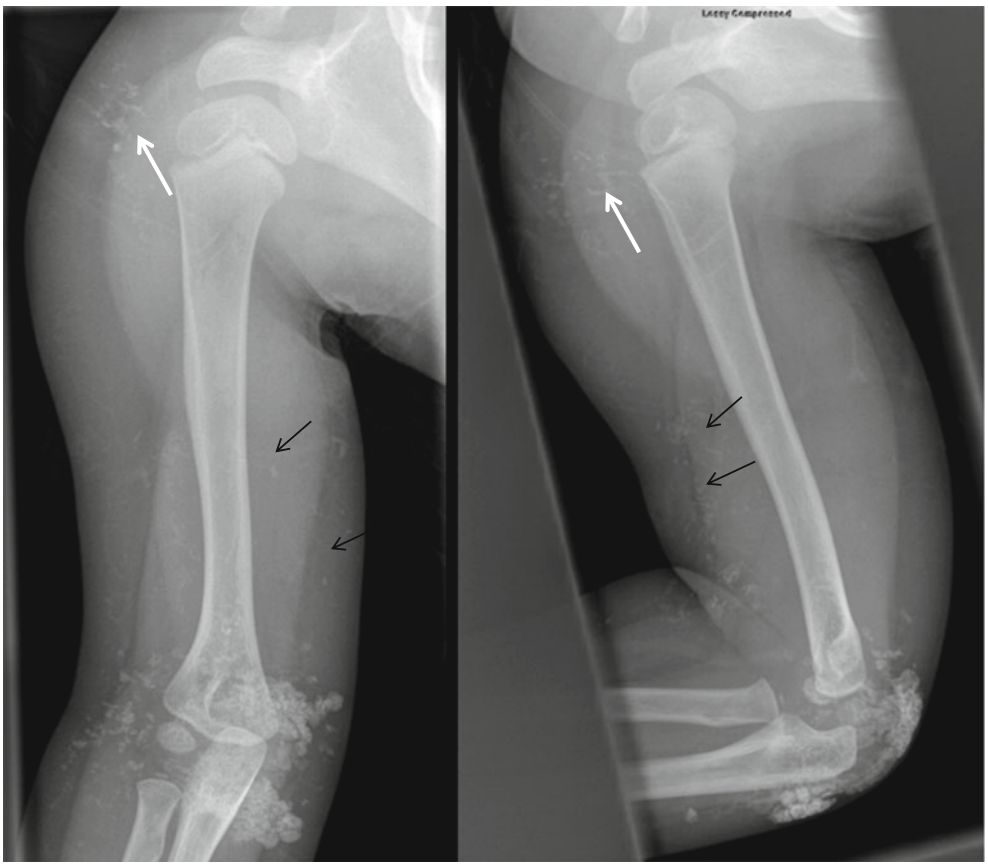

Fig. 31.29 *A 3-year-old girl with dermatomyositis.* A 3-year-old girl with dermatomyositis with extensive soft tissue calcifications of the shoulder (*arrow*) and elbow. Other more faint calcifications are seen around the mid portion of the upper arm (*small black arrows*)

31.6.17 Noninfectious Inflammatory Diseases of the Soft Tissue; Eosinophilic Fasciitis

Fig. 31.30 *A 15-year-old boy with eosinophilic fasciitis.* (**a**, **b**) Axial (**a**) and coronal T2-WI with fat suppression (**b**) demonstrate diffuse bilateral high T2 signal along the fascial planes of the muscles (*arrows*). (**c**) Post-contrast axial T1-WI with fat suppression demonstrates thick enhancement of the fascia (*arrows*). No muscle edema is seen

References

Arnold WD, Hilgartner MW. Hemophilic arthropathy. Current concepts of pathogenesis and management. J Bone Joint Surg Am. 1977; 59:287–305.

Burk Jr DL, Dalinka MK, Kanal E, et al. Meniscal and ganglion cysts of the knee: MR evaluation. AJR Am J Roentgenol. 1988;150:331–6.

Choi JA, Koh SH, Hong SH, et al. Rheumatoid arthritis and tuberculous arthritis: differentiating MRI features. AJR Am J Roentgenol. 2009; 193:1347–53.

Cohen MD, Klatte EC, Baehner R, et al. Magnetic resonance imaging of bone marrow disease in children. Radiology. 1984;151:715–8.

Doria AS. State-of-the-art imaging techniques for the evaluation of haemophilic arthropathy: present and future. Haemophilia. 2010;16 Suppl 5:107–14.

Dorwart RH, Genant HK, Johnston WH, et al. Pigmented villonodular synovitis of synovial joints: clinical, pathologic, and radiologic features. AJR Am J Roentgenol. 1984;143:877–85.

Erdem H, Baylan O, Simsek I, et al. Delayed diagnosis of tuberculous arthritis. Jpn J Infect Dis. 2005;58:373–5.

Goldman AB, DiCarlo EF. Pigmented villonodular synovitis. Diagnosis and differential diagnosis. Radiol Clin North Am. 1988;26: 1327–47.

Gordon BA, Martinez S, Collins AJ. Pyomyositis: characteristics at CT and MR imaging. Radiology. 1995;197:279–86.

Gylys-Morin VM, Graham TB, Blebea JS, et al. Knee in early juvenile rheumatoid arthritis: MR imaging findings. Radiology. 2001;220: 696–706.

Hopkins KL, Li KC, Bergman G. Gadolinium-DTPA-enhanced magnetic resonance imaging of musculoskeletal infectious processes. Skeletal Radiol. 1995;24:325–30.

Howard CB, Einhorn M, Dagan R, et al. Ultrasound in diagnosis and management of acute haematogenous osteomyelitis in children. J Bone Joint Surg Br. 1993;75:79–82.

Iyer RS, Thapa MM, Chew FS. Chronic recurrent multifocal osteomyelitis: review. AJR Am J Roentgenol. 2011;196:S87–91.

Jaramillo D, Treves ST, Kasser JR, et al. Osteomyelitis and septic arthritis in children: appropriate use of imaging to guide treatment. AJR Am J Roentgenol. 1995;165:399–403.

Johnson K, Davis PJ, Foster JK, et al. Imaging of muscle disorders in children. Pediatr Radiol. 2006;36:1005–18.

Kan JH, Young RS, Yu C, et al. Clinical impact of gadolinium in the MRI diagnosis of musculoskeletal infection in children. Pediatr Radiol. 2010;40:1197–205.

Kerr R. Imaging of musculoskeletal complications of hemophilia. Semin Musculoskelet Radiol. 2003;7:127–36.

Ladd PE, Emery KH, Salisbury SR, et al. Juvenile dermatomyositis: correlation of MRI at presentation with clinical outcome. AJR Am J Roentgenol. 2011;197:W153–8.

Lee SK, Suh KJ, Kim YW, et al. Septic arthritis versus transient synovitis at MR imaging: preliminary assessment with signal intensity alterations in bone marrow. Radiology. 1999;211: 459–65.

Legiehn GM, Heran MK. Classification, diagnosis, and interventional radiologic management of vascular malformations. Orthop Clin North Am. 2006;37:435–74, vii–viii.

Llauger J, Palmer J, Roson N, et al. Pigmented villonodular synovitis and giant cell tumors of the tendon sheath: radiologic and pathologic features. AJR Am J Roentgenol. 1999;172:1087–91.

Luck Jr JV, Silva M, Rodriguez-Merchan EC, et al. Hemophilic arthropathy. J Am Acad Orthop Surg. 2004;12:234–45.

Martin S, Hernandez L, Romero J, et al. Diagnostic imaging of lipoma arborescens. Skeletal Radiol. 1998;27:325–9.

Moulton SJ, Kransdorf MJ, Ginsburg WW, et al. Eosinophilic fasciitis: spectrum of MRI findings. AJR Am J Roentgenol. 2005;184: 975–8.

Parmar H, Shah J, Patkar D, et al. Tuberculous arthritis of the appendicular skeleton: MR imaging appearances. Eur J Radiol. 2004;52: 300–9.

Petty RE, Southwood TR, Manners P, et al. International League of Associations for Rheumatology classification of juvenile idiopathic arthritis: second revision, Edmonton, 2001. J Rheumatol. 2004;31: 390–2.

Vilanova JC, Barcelo J, Villalon M, et al. MR imaging of lipoma arborescens and the associated lesions. Skeletal Radiol. 2003; 32:504–9.

Weiss JE, Ilowite NT. Juvenile idiopathic arthritis. Rheum Dis Clin North Am. 2007;33:441–70, vi.